

Article

# Application of Fractional-Order PI Controllers and Neuro-Fuzzy PWM Technique to Multi-Rotor Wind Turbine Systems

Habib Benbouhenni <sup>1</sup>, Nicu Bizon <sup>2,3,4,\*</sup>, İlhami Colak <sup>1</sup>, Phatiphat Thounthong <sup>5,6</sup>  
and Nouredine Takorabet <sup>6</sup>

<sup>1</sup> Department of Electrical & Electronics Engineering, Faculty of Engineering and Architecture, Nisantasi University, Istanbul 34481742, Turkey; habib.benbouhenni@nisantasi.edu.tr (H.B.); ilhami.colak@nisantasi.edu.tr (I.C.)

<sup>2</sup> Faculty of Electronics, Communication and Computers, University of Pitesti, 110040 Pitesti, Romania

<sup>3</sup> Doctoral School, Polytechnic University of Bucharest, 313 Splaiul Independentei, 060042 Bucharest, Romania

<sup>4</sup> ICSI Energy Department, National Research and Development Institute for Cryogenic and Isotopic Technologies, 240050 Ramnicu Valcea, Romania

<sup>5</sup> ICSI Renewable Energy Research Centre (RERC), Faculty of Technical Education, King Mongkut's University of Technology North Bangkok, Bangkok 10800, Thailand; phatiphat.t@fte.kmutnb.ac.th

<sup>6</sup> Group of Research in Electrical Engineering of Nancy (GREEN), University of Lorraine-GREEN, F-54000 Nancy, France; noureddine.takorabet@univ-lorraine.fr

\* Correspondence: nicu.bizon@upit.ro

**Abstract:** In recent years, the methods of controlling electrical machines have been witnessing increasing development to reduce torque and electric current fluctuations in electrical power generation systems from renewable sources such as wind energy. The generation of electric power from wind plants imposes the need for an efficient and more robust method in order to obtain fewer ripples in active and reactive power. In this work, a new fractional-order proportional-integral (FOPI) controller and intelligent PWM (IPWM) technique are proposed to control an existing asynchronous generator (AG) in variable-speed multi-rotor wind turbines (VSMRWTs). This proposed method depends on combining or using two methods, namely nonlinear area and fractional calculus, to obtain a more robust method and to reduce current and torque ripples. In the framework of this study, the electric power generation system consists of a 1.5 MW AG and VSMRWTs. The AG is controlled using a simpler and easily accomplished method called direct vector control, based on FOPI controllers and the IPWM technique (DVC-FOPI-IPWM). The maximum power point tracking (MPPT) method is used to generate the maximum energy from the VSMRWTs. The proposed DVC-FOPI-IPWM technique is modeled in the Matlab/Simulink platform to obtain good quality current and active power. Simulation results show that the proposed strategy reduces the ripples of torque, current, and active power compared to the classical technique. Moreover, the reduction ratio is about 85%, 99%, and 93.33% for the current, active power, and torque, respectively.

**Keywords:** renewable sources; fractional-order proportional-integral controller; intelligent pulse width modulation; variable-speed multi-rotor wind power; torque ripple; asynchronous generator; maximum power point tracking



**Citation:** Benbouhenni, H.; Bizon, N.; Colak, I.; Thounthong, P.; Takorabet, N. Application of Fractional-Order PI Controllers and Neuro-Fuzzy PWM Technique to Multi-Rotor Wind Turbine Systems. *Electronics* **2022**, *11*, 1340. <https://doi.org/10.3390/electronics11091340>

Academic Editor: J. C. Hernandez

Received: 21 March 2022

Accepted: 20 April 2022

Published: 22 April 2022

**Publisher's Note:** MDPI stays neutral with regard to jurisdictional claims in published maps and institutional affiliations.



**Copyright:** © 2022 by the authors. Licensee MDPI, Basel, Switzerland. This article is an open access article distributed under the terms and conditions of the Creative Commons Attribution (CC BY) license (<https://creativecommons.org/licenses/by/4.0/>).

## 1. Introduction

In recent times, the demand for world electric energy has been increasing, especially in more industrialized countries such as China and the USA. Wind energy is among the different types of renewable energy sources that are widely used. This type of renewable energy offers a realistic alternative to electric power production. Therefore, to ensure optimal utilization of this energy, different control strategies have been well studied in the literature [1–5].

In the field of wind energy, there are several kinds of wind powers that have been used to generate electric power. As it is known to the private and public, the single-rotor

turbine is the most widely used and famous [6]. This type of turbine has several problems, especially concerning the part of the energy gained from wind. In addition, in the case of wind farms, there is wind generated by the turbines, and the energy gained from the wind is affected by this wind generated by the wind farms [7]. All these problems made researchers and those interested in the energy field search for a solution to these problems. Among the solutions proposed in this field is the multi-rotor turbine.

A multi-rotor wind turbine is a wind turbine that contains several wind turbines in order to obtain the largest amount of wind energy [8]. However, the wind generated in the case of wind farms must be overcome. The dual-rotor wind turbine is the most studied and used type in the field of electric power production, and this is due to the performances of this system and the results obtained [9]. In addition, the production cost of this system is lower compared to that of a system with a multi-rotor wind turbine [10]. Many studies have been carried out in this field to control twin-rotor turbines [11–15]. In [16], a multi-rotor wind turbine system with multi-generator drive trains is presented. The proposed turbine uses a multi-rotor configuration with five rotors arranged in a star shape configuration. The use of this technology has many goals, including reducing the size of the wind farm and thus reducing the cost of industrialization. Moreover, this technology aims to increase the proportion of electrical power output. As it is known, wind affects the structure of turbines and generates vibrations. Moreover, heavy loads on the structure are all negative factors that affect the turbines. These problems increase the requirements for periodic maintenance and thus contribute to a high cost of energy production, and this is not desirable [17].

Several generators can be used with this new technology, as it is possible to use an asynchronous generator as well as a synchronous generator. However, the asynchronous generator is the most widely used with this new technology, and this is due to the advantages and high efficiency of this type of generator, especially in the case of variable wind speed [18]. The authors of [19] implemented a nonlinear direct field-oriented control on an induction generator system using terminal synergetic control, in which the proposed strategy was to minimize power ripples. Despite the improvements achieved, which were enhanced in comparison with a traditional integral-proportional (IP), the main drawback of the synergetic controls is the increase in power consumption. In [20], a new nonlinear method is used to control an asynchronous generator (AG) in a multi-turbine system. In this work, the characteristics and effectiveness of direct flux and torque control were improved by using third-order sliding mode control (TOSMC). The results show that the characteristics of the designed strategy improve the quality of the active power produced by the dual-rotor wind turbine system. Another advanced approach is the usage of neural network algorithms (NNAs) for the tuning of a TOSMC technique of the induction generator-based multi-rotor wind turbine (MRWT) system. According to the study generated by the authors of [21], with the latter mentioned structure, the results were contrasted against a fixed-gain controller, and significant improvements were observed. However, one of the main drawbacks of using NNA to improve the nonlinear method of the AG is that many input variables must be used to obtain an accurate result. Another nonlinear control strategy used to control the AG integrated into the MRWT system is second-order sliding mode control (SOSMC), which is known for its robustness against disturbances and uncertainties for large-scale systems as well as its practicality in terms of implementation [22]. The performance and efficiency of the generator can be increased by using nonlinear methods and even by using a combination of several methods for controlling a system, as the authors of [23] did in their study. In this work, a new linear technique is proposed based on the integration of both sliding mode control and synergetic control. Through the results of the digital simulation, there is a noticeable improvement in the behavior of the generator in terms of dynamic response. In fact, it is recommended over techniques such as synergetic control [24]. In [25], the authors combined fractional-order control and a terminal sliding mode controller to control an asynchronous generator placed in a wind system. The proposed method improves the quality of electrical energy compared to the classical method. Moreover, the proposed technique minimizes the total harmonic distortion (THD) of the

stator current of the AG compared to the traditional strategy. Durability is among the advantages of this proposed method, as this proposed method is more robust compared to the proposed method. Moreover, the proposed method reduces effective and reactive power fluctuations compared to the classical method. A second-order continuous sliding mode controller and fractional-order control were combined to minimize the active power and current of the asynchronous generator-based wind turbine system [26]. Another method is suggested in [27], in which a fuzzy-genetic algorithm and direct power control were combined to control the effective and reactive power of the AG-based wind turbine. The results show the effectiveness of the proposed method in reducing ripples and improving the quality of effective power compared to the classical method. A proportional-integral (PI) controller based on fractional-order control was used to control distributed generation (DG) inverter control [28]. Moreover, in addition to using a fractional-order PI controller, a space vector modulation technique was used to control the active and reactive power of the DG inverter.

In the wind power generation system, there are several faults affecting it, including those that are electrical and mechanical. These faults affect the torque and affect the quality of the electrical energy generated by the generator. In addition, these defects increase the production bill and maintenance cost. In [29], the performance of a wind power system in the event of failures in the lubrication system is shown. Moreover, a procedure is proposed to detect malfunctions caused by the lubrication system. This failure of the lubrication system makes the maximum power point (MPP) of the wind system smaller than that of normal operation. The difference between the actual and simulated (estimated) output power of the wind system is an indication of the failure of the lubrication system. Additionally, two different methods are suggested in [30] to control the asynchronous generator, in which the first is an integer-order PI controller and the second is a fractional-order PI (FOPI) controller. The study compares these two methods in terms of dynamic response, ripple ratio for effective power, and THD value of electric current for doubly-fed induction generator (DFIG)-based marine tidal current applications. In [31], a FOPI controller is a better candidate in wind energy applications compared to the integer-order PI controller. A fractional-order PI controller is employed to control the energy exchange between a high-temperature superconductor and the system by controlling the duty cycle of the DC chopper interfacing the high-temperature superconductor with the DC link [32]. Rating the high-temperature superconductor and the parameters of the FOPI controller is precisely calculated using the harmony search optimization technique in order to regulate the DFIG-generated power and to improve its fault ride-through capability during disturbance events. The results obtained using the FOPI controller are compared with the results obtained using the conventional PI controller. The results reveal the ability of the FOPI controller to improve the performance of DFIG-based wind turbines during wind gusts and short circuit faults at DFIG plants. In [33], fractional-order PI controllers are simultaneously applied in the internal and external control loops of the RSC to improve DFIG active power, rotor speed, and rotor current profiles by occurring with various balanced and unbalanced transient faults. The results obtained from the FOPI controller are compared with those of the PI controller, and the results show how effective the FOPI controller is in improving the quality of effective power.

In the field of control, many methods have provided satisfactory results for controlling electrical machines and especially for controlling electrical generators. Research has mostly focused on single-rotor wind turbines. As demonstrated in [34], this type of turbine gives less mechanical energy. Accordingly, the energy gained from wind is weak, and this is undesirable.

There is a need to gain more energy from wind to rotate the asynchronous generator, so the technical way to obtain optimum energy from wind is the use of a multi-rotor wind turbine. The latter helps to gain more wind energy. In addition, control of generators is essential, as methods of controlling generators are of great importance for the quality of

the electric current produced. As is known, the use of direct torque control to control the asynchronous generator is better than the use of the FOC method.

In this paper, a wind electric power generation system using a multi-rotor wind turbine is studied. An asynchronous generator is used in the studied system to generate electric current due to its durability and low cost. In this paper, new uses include both the proposed method of the PWM technique based on the use of artificial intelligence, as well as the use of a new design of PI controller based on fractional-order control, in which the proposed method for the fractional-order PI controller is different from that of published works [35–39]. Moreover, this work is a development of the direct vector control (DVC) method. The DVC strategy based on the intelligent PWM technique and the fractional-order PI controller is proposed to control the asynchronous generator and to obtain fewer ripples for current, torque, and active power. Additionally, the proposed DVC technique is more robust than the traditional DVC strategy with a PI controller.

The methods proposed in this paper are first-time methods proposed for controlling an asynchronous generator integrated into a multi-rotor wind turbine system. In addition, the intelligent PWM (IPWM) technique is used to obtain a fixed-frequency signal at the output of the inverter, and the proposed fractional-order PI controller is used to obtain a fast dynamic response and to improve the performance of the asynchronous generator integrated into the multi-rotor wind turbine system. The proposed DVC method and the advantages of the proposed FOPI controller and IPWM technique are given in this paper.

In order to confront and overcome the problems and shortcomings of the DVC method, this paper presents its main contributions as follows:

- Numerical simulation results are presented to validate the advantages of the proposed DVC method.
- The PI controller is among the most important and most widely applied controllers in the field of control of electric generators. However, for this kind of controller, several defects can be improved or eliminated by using artificial intelligence or fractional calculus. It emerges that the proposed fractional-order PI controller is more convenient than the classic PI controller.
- The IPWM technique is proposed as a better solution than the classical PWM method to control the inverter to obtain a signal at its output with a fixed frequency.
- The proposed DVC method is a development of [40] because it gives a new design and optimum solution to control an asynchronous generator using the method based on the new FOPI controller, whereas the classic DVC method is based on the PI controller, which makes the current quality lower. For the same reason, the proposed DVC method has a higher probability of obtaining a higher quality of electric current and active power than the previous solution.

In order to understand the work performed in this paper, the design, testing, and validation stages of the proposed DVC strategy are shown in Figure 1.

This work contains the following main themes: The Section 1 gives an introduction to this work, mentioning its contributions and goals. In the Section 2, the mathematical form of the proposed system consisting of a generator and an MRWT system for the generation of electrical energy is discussed alongside how this is performed. In the Sections 3 and 4, the proposed IPWM technique and a new fractional-order PI controller are discussed, respectively. The classical DVC method is briefly discussed in the Section 5. The Section 6 is dealt with in minute detail concerning the proposed DVC-FOPI-IPWM technique used in the dual-rotor wind energy system. In the Section 7, the simulated results of the proposed DVC-FOPI-IPWM method are given, where it is compared with the classical DVC method. Finally, all the conclusions reached from this work are collected in the Section 8.

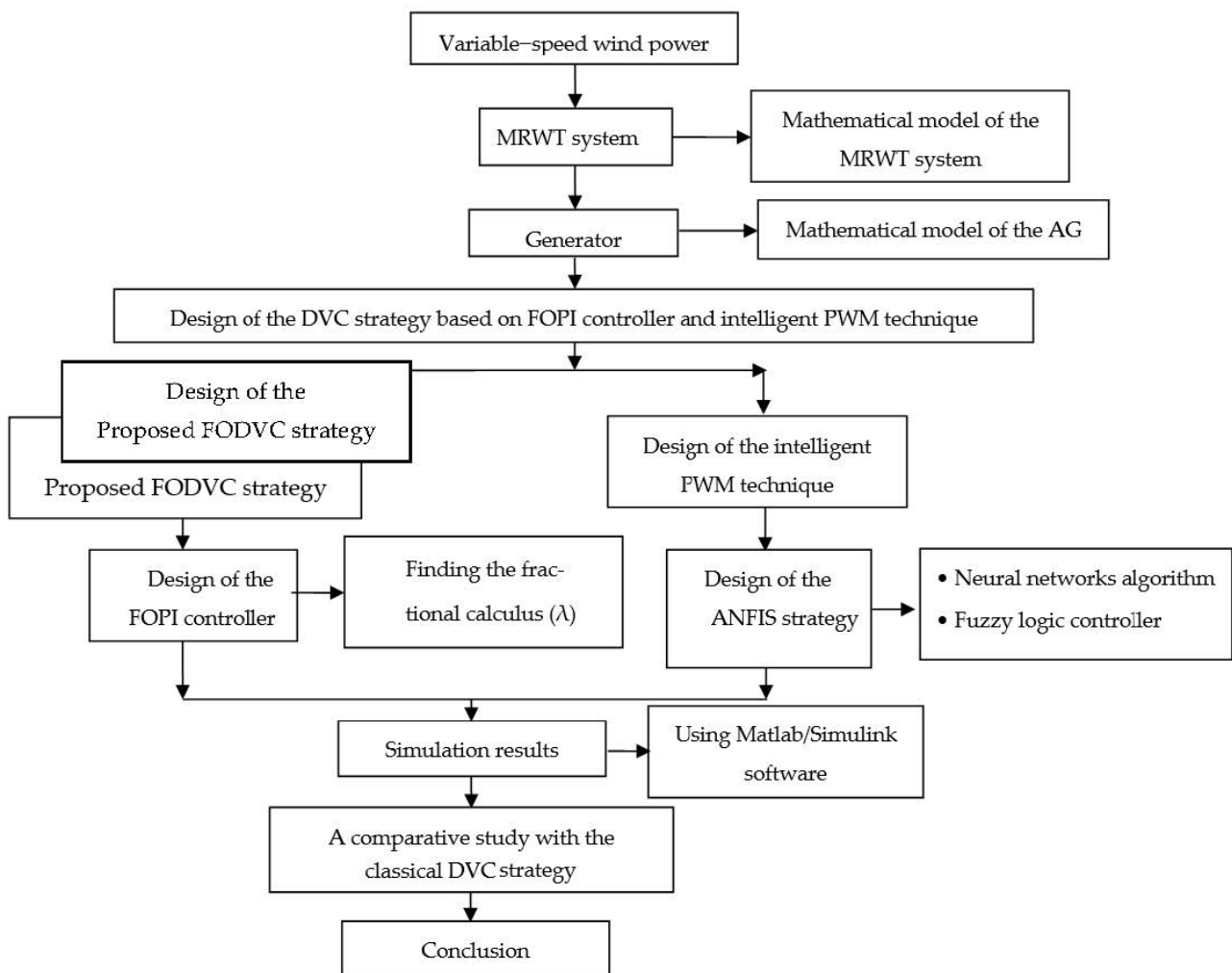


Figure 1. Diagram for proposed DVC strategy.

## 2. Multi-Rotor Wind Turbine System

Wind energy is one of the most important power sources used today for several reasons, including a low cost of production and an absence of toxic gases. In addition, to generate electricity from wind, we use wind farms. The latter contain wind turbines, which convert wind energy into mechanical energy. The acquired mechanical energy is used to rotate the generator, for example, as an asynchronous generator, thus producing electrical energy.

In conventional farms, a single-rotor turbine is used. This type of turbine has several problems. The energy gained from wind is not great by using this type of turbine [41]. Moreover, this type of turbine is affected by the wind that is generated by wind farms [42]. In order to overcome these difficulties and to increase the value of the mechanical energy gained from wind, it is necessary to develop a traditional turbine. Among the solutions proposed in the past few years is the adding of a second turbine to the main turbine, which doubles the value of the energy gained from the wind. In this way, new technology is created to generate electricity from wind with a multi-rotor turbine. This type has been studied in several scientific works [43–46].

In this work, we study an MRWT system for the generation of electric energy from wind. Figure 2 illustrates the electrical power generation system used in this work, where  $P_s^*$  and  $Q_s^*$  represent the references for active and reactive power. In this way, this system is almost the same as the normal system used to generate electricity from wind, and the difference lies in the use of an MRWT system only. The use of an MRWT system leads to

an increase in the mechanical energy gained from wind, thus obtaining a speed (torque) sufficient to rotate the asynchronous generator [9].

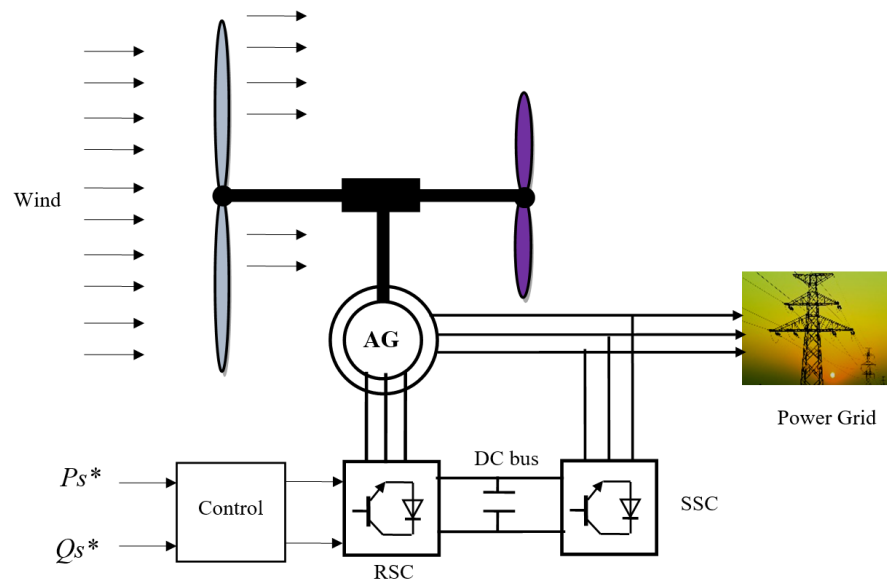


Figure 2. Structure of MRWTS.

In these new wind turbines, two rotors are used. The first is the main rotor, and the second is the auxiliary rotor [8]. The use of rotors leads to the complexity of controlling this type. Additionally, this type of turbine is expensive and has a large number of mechanical parts compared to the old type. Moreover, this new technology requires more maintenance than the old technology [10].

In an MRWT system, the output torque is the sum of the torques of the main and secondary turbines, and the same applies to the mechanical energy gained from wind. The total torque of the turbine can be expressed by relationship (1) [13]:

$$T = T_m + T_a \tag{1}$$

where  $T_a$  and  $T_m$  are the torque of the auxiliary and main rotors [14,15]:

$$\begin{cases} T_a = \frac{C_p}{2\lambda_a^3} \rho \cdot \pi \cdot R_a^5 \cdot w_a^2 \\ T_m = \frac{C_p}{2\lambda_m^3} \rho \cdot \pi \cdot R_m^5 \cdot w_m^2 \end{cases} \tag{2}$$

The energy gained from the dual-rotor wind turbine is the energy generated by the main wind turbine in addition to the mechanical power produced by the secondary wind turbine, and it is explained by relationship (3):

$$P = P_m + P_a \tag{3}$$

where  $P_a$  and  $P_m$  are the mechanical power of the auxiliary and main rotors, respectively.

Through Equation (3), the torque relationship can be clarified for each of the main and secondary wind turbines. It can be seen that the torque for the two wind turbines is related to both air density ( $\rho$ ), mechanical speed ( $w_a$  and  $w_m$ ), power coefficient ( $C_p$ ), tip speed ratio ( $\lambda_a$  and  $\lambda_m$ ), and the blade radius of the auxiliary and main rotors ( $R_m$  and  $R_a$ ).

The relationship of the power coefficient almost remains the same as in the ordinary turbines (single-rotor). Equation (4) represents the relationship through which this coefficient can be calculated for a dual-rotor wind turbine.

$$C_p(\lambda, \beta) = \frac{1}{\lambda + 0.08 \cdot \beta} - \frac{0.035}{\beta^3 + 1} \tag{4}$$

Equation (4) shows that the pitch angle has a large effect on the power coefficient and therefore on the power gained, where the smaller that the pitch angle is, the greater that the coefficient is; therefore, the energy gained from the wind is large. Additionally, the coefficient's power is affected by the value of the tip speed ratio. We find that the higher that the tip speed ratio is, the lower that the tip speed ratio value is; thus, the value of the energy gained from the dual-rotor wind turbine is lower and vice versa.

The tip speed ratios of the main and auxiliary wind turbines are given by Equation (5) for a dual-rotor wind turbine:

$$\begin{cases} \lambda_a = \frac{w_a \cdot R_a}{V_1} \\ \lambda_m = \frac{w_m \cdot R_m}{V_m} \end{cases} \quad (5)$$

As is well known, determination depends on the wind speed of the auxiliary and main wind turbines ( $V_1$  and  $V_m$ ), the blade radius of the auxiliary and main wind turbines, and the mechanical speed of the auxiliary and main wind turbines.

Wind speed ( $V_w$ ) varies from the main turbine to the secondary. To calculate wind speed in the secondary turbine, we use relationship (6). This relationship is demonstrated in [12].

$$V_x = V_w \cdot \left( -\frac{1 - \sqrt{(1 - C_T)}}{2} \left( \frac{2x}{\sqrt{1 + 4x^2}} + 1 \right) + 1 \right) \quad (6)$$

Wind speed in the auxiliary wind turbine is related to the wind speed before the main turbine ( $V_x$ ), the distance from the auxiliary rotor disk ( $x$ ), and a thrust coefficient ( $C_T$ ). In the turbine used in this work, the distance between the main and auxiliary turbines is 15 m, and the thrust coefficient is 0.9 [10–14].

Among the components of the electricity generation system using dual-rotor wind turbines, we find the asynchronous generator and two inverters. Inverters are used to feed the rotor of the asynchronous generator [6]. The first inverter aims to convert alternating current to continuous, whereas the second inverter converts direct current to alternating voltage.

To study this system, it is necessary to have the mathematical form of the AG-based MRWT system. As is well known, the generator has two parts; one is static, and the other is movable. The static part is called the stator and contains coils, and the rotating part is called the rotor, which is also composed of coils. The mathematical model of the AG uses the Park transform, in which both direct and quadrature flux and voltage are given. Equations (7) and (8) represent the direct and quadrature rotor voltage and flux of the AG, respectively [7]:

$$\begin{cases} V_{dr} = R_r I_{dr} + \frac{d}{dt} \varphi_{dr} - \omega_r \varphi_{qr} \\ V_{qr} = R_r I_{qr} + \frac{d}{dt} \varphi_{qr} + \omega_r \varphi_{dr} \end{cases} \quad (7)$$

$$\begin{cases} \varphi_{dr} = L_r I_{dr} + M I_{ds} \\ \varphi_{qr} = L_r I_{qr} + M I_{qs} \end{cases} \quad (8)$$

Through these two equations, the direct and quadrature rotor voltage ( $V_{dr}$  and  $V_{qr}$ ) is related to the direct and quadrature flux ( $\varphi_{dr}$  and  $\varphi_{qr}$ ), the direct and quadrature rotor current ( $I_{dr}$  and  $I_{qr}$ ), and the resistance value ( $R_r$ ). Additionally, the flux is related to both direct and quadrature rotor current and to the rotor/mutual inductance of the rotor ( $M$  and  $L_r$ ).

The direct and quadrature stator voltages ( $V_{ds}$  and  $V_{qs}$ ) of the generator are shown in Equation (9):

$$\begin{cases} V_{ds} = R_s I_{ds} + \frac{d}{dt} \varphi_{sd} - \omega_s \varphi_{qs} \\ V_{qs} = R_s I_{qs} + \frac{d}{dt} \varphi_{qs} + \omega_s \varphi_{ds} \end{cases} \quad (9)$$

These voltages are concerned with quadrature and direct stator flux ( $\varphi_{ds}$  and  $\varphi_{qs}$ ), and this flux can be expressed by Equation (10) [12]:

$$\begin{cases} \varphi_{ds} = L_s I_{ds} + M I_{dr} \\ \varphi_{qs} = L_s I_{qs} + M I_{qr} \end{cases} \quad (10)$$

Equation (11) represents the mechanical equation of the AG-based MRWT system:

$$T_e - T_r = J \frac{d\Omega}{dt} + f\Omega \quad (11)$$

This equation shows the relationship between torque and mechanical rotor speed, and it explains how velocity changes in relation to torque. Through this equation, the change in mechanical rotor speed ( $\Omega$ ) is related to the load torque ( $T_r$ ), electromagnetic torque ( $T_e$ ), viscous friction coefficient ( $f$ ), and inertia ( $J$ ).

Torque is given by Equation (12) [3,5]:

$$T_e = \frac{3}{2} p \frac{M}{L_s} (\varphi_{sq} I_{rd} - \varphi_{sd} I_{rq}) \quad (12)$$

Equation (12) shows that change in torque is related to change in both direct/quadrature rotor current and direct/quadrature stator flux. Moreover, change in torque can be performed by changing the number of pole pairs ( $p$ ).

Active and reactive power can be expressed by Equation (13):

$$\begin{cases} P_s = \frac{3}{2} (+V_{qs} I_{qs} + V_{ds} I_{ds}) \\ Q_s = \frac{3}{2} (+V_{qs} I_{ds} - V_{ds} I_{qs}) \end{cases} \quad (13)$$

Through Equation (13), it is possible to control the active and reactive power from direct and quadrature stator current and voltage. A change in stator voltages or stator current leads to a change in both the reactive power and the active power.

There are several ways to control the AG-based MRWT system, some of which are linear and some of which are nonlinear techniques. Among the most popular methods used in controlling electrical machines, there is DTC strategy, DPC technique, and vector control. In this work, the focus is on direct vector control, and this is because of its simplicity and ease of implementation. In this work, a new algorithm is given for this method, depending on both the proposed IPWM technique and the fractional-order PI controller. The proposed IPWM technique is explained in the third part of the article, and in the fourth chapter, a new fractional-order PI controller is addressed.

### 3. Proposed IPWM Technique

In electrical machines, the PWM technique is among the oldest and most widely used modulation methods for controlling electric motors due to its simplicity and ease of implementation [47]. Figure 3 (on the left) represents the conventional PWM technique of the two-level inverter. In the PWM technique, two signals of different frequencies are compared, and a triangular signal with a frequency much greater than the frequency of the sinusoidal signal that represents the network's voltage is used. Moreover, three hysteresis controllers are used to create the control signals ( $S_a$ ,  $S_b$ , and  $S_c$ ) of the inverter. The use of these conventional controllers causes variable frequencies at the output level of the inverter, where the inverter gives a sinusoidal signal of variable frequencies. Variable frequency is a major problem that affects the performance of electrical machines such as asynchronous generators. In addition, the use of a sinusoidal signal with variable frequencies leads to a decrease in the life of electrical machines [48].

In order to overcome this problem and to obtain a sinusoidal signal with a fixed frequency, a method of artificial intelligence was used. In this proposed IPWM technique, classical hysteresis comparators are compensated by an intelligent method based on an adaptive neuro-fuzzy inference system (ANFIS) algorithm. Using this method leads to obtaining a high-quality sinusoidal signal (fixed frequency), thus overcoming the disadvantages of the traditional PWM method. Figure 3 (on the right) represents the proposed IPWM technique in this work for controlling the inverter of the asynchronous generator. Through this figure, the proposed IPWM method is reverted to the classical PWM method with the substitution of the hysteresis controller by the ANFIS algorithm. In addition, the

proposed IPWM method is simple and uncomplicated, does not require a specialist, and can be easily accomplished.

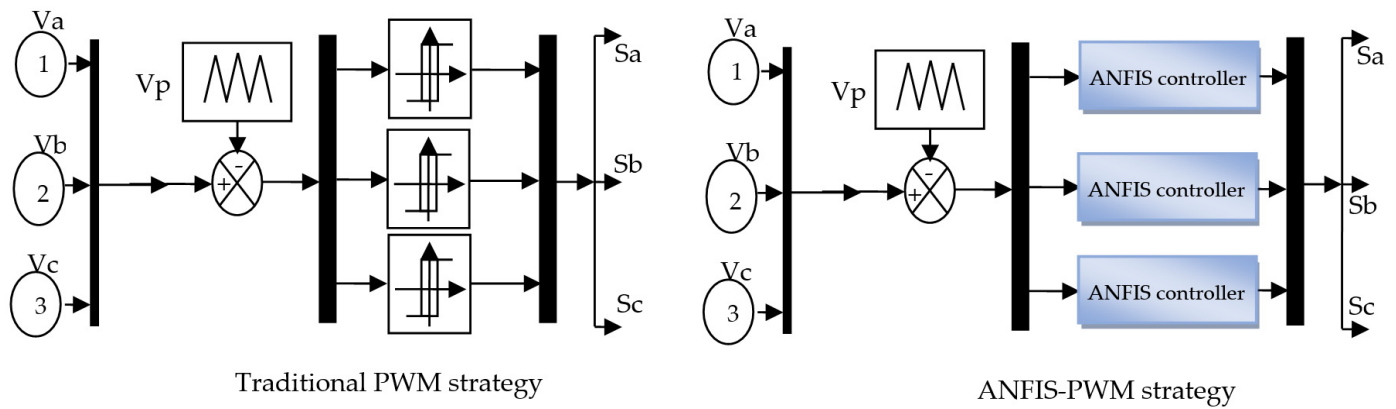
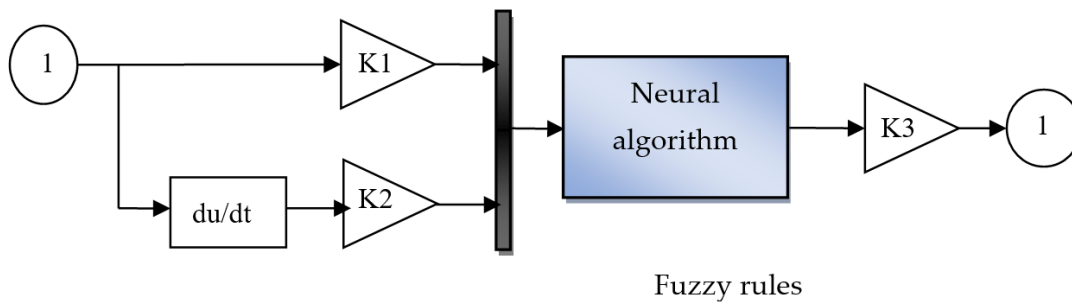


Figure 3. Structure of the traditional PWM strategy (left) and proposed IPWM strategy (right).

The ANFIS algorithm is one of the most important algorithms of artificial intelligence spread in recent times. In this type of algorithm, the advantages of neural networks are combined with the advantages of fuzzy logic. In this algorithm, rules are compensated by neural networks [49]. Figure 4 represents the internal structure of the ANFIS algorithm.



Fuzzy rules

where NL is defined as negative large, ZR is zero, and PL, PM, and PS are positive large, positive medium, and positive small, respectively. NM and NS are negative medium and negative small, respectively.

e	NL	NM	NP	EZ	PS	PM	PL
$\Delta e$	NL	NL	NL	NL	NM	NP	EZ
NL	NL	NL	NL	NL	NM	NP	EZ
NM	NL	NL	NL	NM	NP	EZ	PS
NP	NL	NL	NM	NP	EZ	PS	PM
EZ	NL	NM	NP	EZ	PS	PM	PL
PS	NM	NP	EZ	PS	PM	PL	PL
PM	NP	EZ	PS	PM	PL	PL	PL
PL	EZ	PS	PM	PL	PL	PL	PL

Figure 4. The internal structure of ANFIS algorithm.

Among the advantages of this algorithm are that it is simple, unrelated to the system, and can be applied and implemented easily [50]. However, among its downsides, there is no mathematical theory that explains how each of the rules selects the number of neurons within the middle layer of the neural network. Therefore, this algorithm depends on the experience of the user and on the extent of its application to automated systems. On the other hand, the ANFIS controller is very understandable and easy. It can also be applied to any system, regardless of its complexity, as it is not related to the studied system. The ANFIS controller is able to provide the most effective solution to complex issues. The

system can be easily modified to improve or modify performance. Moreover, the ANFIS controller helps deal with engineering uncertainties.

The rules shown in Figure 4 were used to implement the ANFIS algorithm. Regarding the membership functions (MFs) used to implement the ANFIS algorithm, they are shown in Figure 5, where the same functions are used in the two inputs (error and change in error). In order to give more accuracy and to obtain excellent results, 49 rules were used. In addition, these rules were chosen based on experience, expert knowledge, and the dynamics of the process, whereby the greater that the number of these rules is, the slower that the system is.

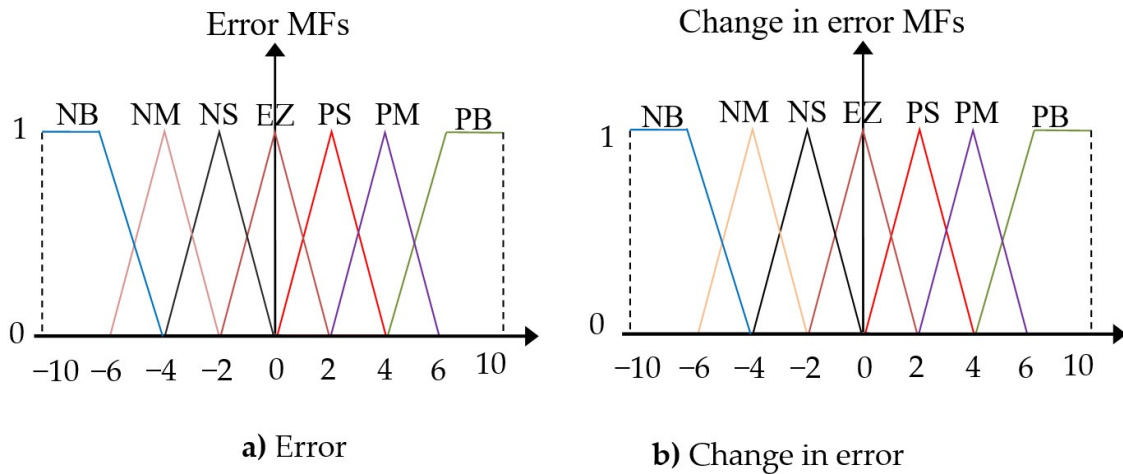


Figure 5. Membership functions.

Regarding the neural networks, eight cells were selected in the inner layer, and in the outer and front layer, one cell and two cells were selected, respectively. The characteristics of the neural network used to perform ANFIS algorithms are shown in Table 1. In order to implement the neural networks, a conjugate gradient with Beale–Powell restarts was used. The following functions were also used to obtain the neural networks: tansig, purelin, and traincgb.

Table 1. Features of neural networks used.

Parameters	Values
Training	Conjugate gradient with Beale–Powell restarts
Train Param.eposh	100
Coeff. of acceleration of convergence(mc)	0.9
Number of neurons in hidden layer	50
Performances	Mean Squared Error (mse)
Train Param.mu	0.8
Functions of activation	Tansig, purelin, traincgb
Number of neurons in layer 1	2
Train Param.goal	0
Train Param.show	50
Train Param.Lr	0.05
Number of neurons in layer 2	1

The ANFIS algorithm training of the hysteresis comparators is shown in Figure 6. Figure 7 shows the training plot of the ANFIS algorithm for the hysteresis comparators. In this figure, the best training performance is  $9.0749 \times 10^{-5}$  at epoch 10 for traditional hysteresis comparators. The error plot of the ANFIS algorithm is shown in Figure 8, where the targeting field is  $[-140 -40]$ , the training value is  $R = 1$ , and the output for hysteresis comparators is given by  $output = 1 \times Target + 0.00014$ . Additionally, gradient, mu, and

validation checks are shown in Figure 9, and they represent the characteristics of the ANFIS algorithm of the traditional hysteresis comparators. In this figure, the best gradient, step size, and validation checks are 0.0040475, 0, and 0 at epoch 11, respectively.

The internal structure of the neural network of the ANFIS controller is shown in Figure 10. In this figure, the inner form of a neural network consists of two main parts: Layer 1 and Layer 2.

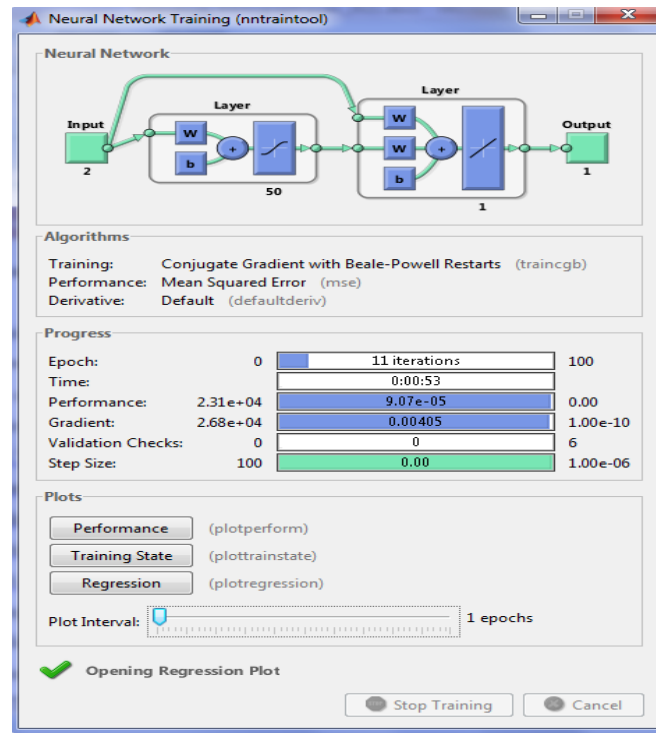


Figure 6. Neural network training.

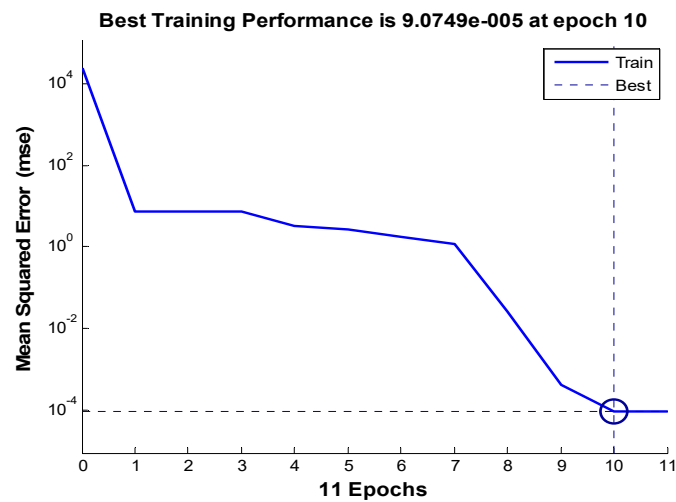


Figure 7. Training plot.

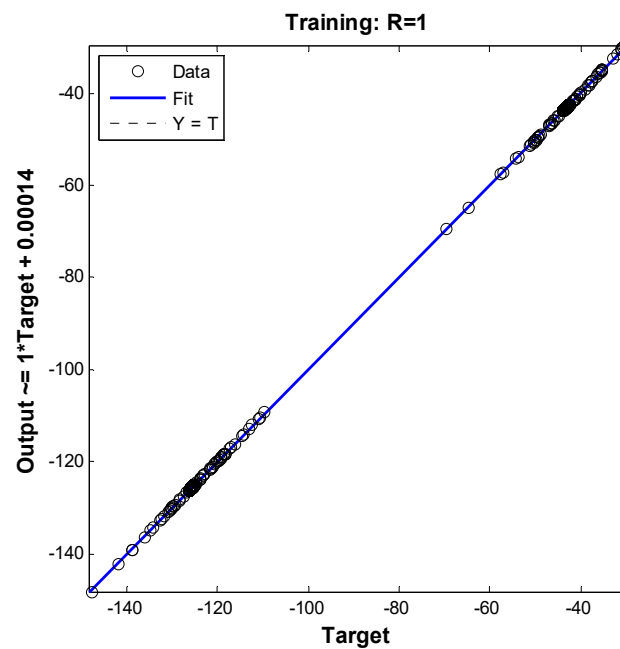


Figure 8. Error plot of the ANFIS controller.

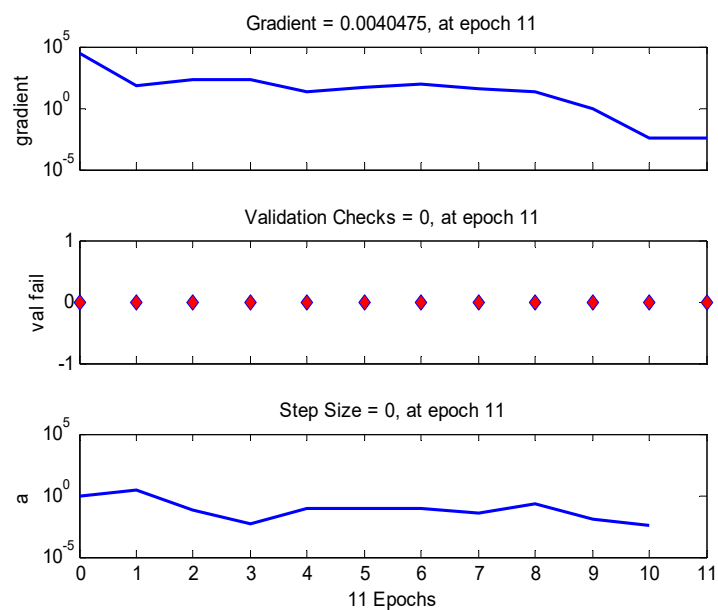


Figure 9. Characteristics of the neural network for hysteresis controller.

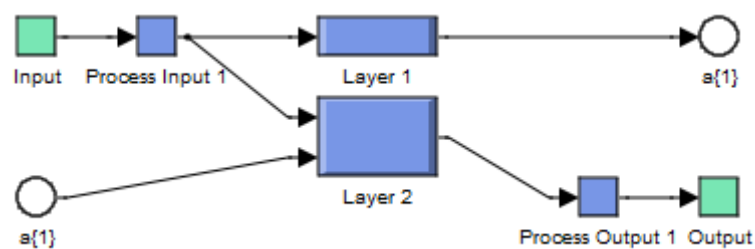


Figure 10. Structure of the neural controller of the ANFIS controller.

#### 4. Proposed Fractional-Order PI Controller

In the fields of control theory and dynamical systems, a fractional-order system is a dynamical system that can be modeled by a fractional differential equation containing derivatives of non-integer order. Such systems are said to have fractional dynamics. However, fractional-order calculus (FOC) is one of the most popular and emerging mathematics branches that deals with differentiation and integration of real or complex order [51]. Moreover, the FOC technique provides efficient tools for many situations related to chaotic behavior, infinite memory, and fractal dimensions [52]. Additionally, fractional calculus is a mathematical method for improving the performance of classical methods, and it was used to improve the performance and effectiveness of the traditional PI controller. The use of this method gives great effectiveness in automated systems, especially in electrical power generation systems [53–56].

A combination of fractional calculus and the PI controller results in the creation of the FOPI controller, which is more robust compared to the classical PI controller. Using the FOPI method in wind power generation systems leads to a significant improvement in the quality of the current and the active power. Equation (14) shows the mathematical form of the FOPI controller, which is frequently used in wind power generation systems [51]:

$$u = K_p \cdot e(t) + K_i \cdot D_t^{-\lambda} \cdot e(t) \quad (14)$$

where  $K_i$  is the integrating constant,  $e(t)$  is the error,  $K_p$  is the proportional constant, and  $\lambda$  is the fractional order of the integrating action.

The difference between the FOPI controller and the traditional PI controller lies in the use of fractional calculus ( $D_t^{-\lambda}$ ). By changing the value of the fractional order, the automated systems are well controlled, i.e., a good way to smooth the results is possible. In the case of  $\lambda = 1$ , the FOPI controller is the traditional PI controller.

In this work, we present a new form of fractional-order PI controller in order to improve the performance and efficiency of the DVC strategy of the asynchronous generator-based multi-rotor wind turbine system. In this part, a new form of the FOPI controller is given in order to reduce torque and active power ripples. In addition, the quality of the current is improved by decreasing the value of the THD. The proposed FOPI controller is different from the proposed FOPI controller in [51,53–56].

The proposed mathematical form for the FOPI controller is shown in Equation (15):

$$w = (K_p \cdot e(t) + K_i \cdot e(t))^{-\lambda} \quad (15)$$

where the fractional calculus of the FOPI controller is changed to calculus that is both integral and proportional. This suggested method is simple and easy. Additionally, the proposed FOPI controller can be applied to any linear or non-linear system. Figure 11 shows the proposed FOPI controller in this paper. Based on this figure, the proposed FOPI controller is a simple structure and can be easily accomplished. Furthermore, the response of the proposed FOPI controller can be smoothed out by changing only one element ( $\lambda$ ). Moreover, this proposed FOPI controller is not complicated.

This designed FOPI technique is used in this paper in order to improve the quality of both the current and the active power of an asynchronous generator controlled by direct vector control. In the next section of the paper, the necessary information and explanation of the DVC strategy are given.

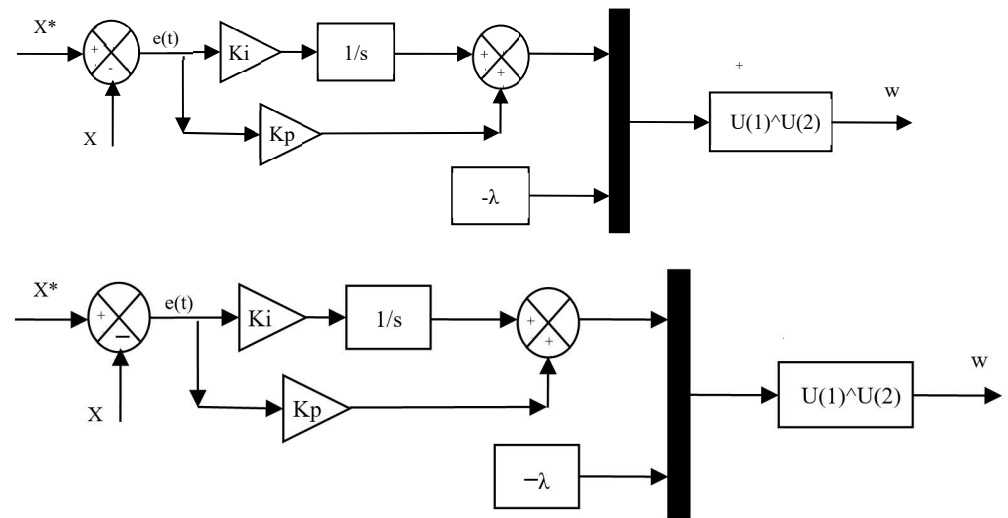


Figure 11. Proposed FOPI controller.

### 5. Direct Vector Control

Traditionally, the DVC strategy is among the easiest and most widely used control methods that are available, and it depends on the use of a traditional PI controller, as we use this method in our PI controller. The use of the latter leads to a fast dynamic response and to a reduction in ripples at the level of both current and torque compared to hysteresis comparators. However, simplicity is one of the most important features of this strategy. The working principle of the classical DVC strategy is explained in [57]. In this paper, this method is used to control a large power 1.5 MW AG-based MRWT system. Equations (16)–(19) illustrate the working principle of this method, which is based on the stator flux given by Equation (16):

$$\varphi_{ds} = 0 \text{ and } \varphi_{qs} = \varphi_s \tag{16}$$

In an asynchronous generator, the stator flux is related to stator voltage. The expressions for both direct and quadrature voltages are shown in Equation (17):

$$\begin{cases} V_{qs} = V_s = \omega_s \cdot \varphi_s \\ V_{ds} = 0 \end{cases} \tag{17}$$

Based on Equations (16) and (17), the direct and quadrature currents are represented in Equation (18):

$$\begin{cases} I_{qs} = -\frac{M}{L_s} I_{qr} \\ I_{ds} = -\frac{M}{L_s} I_{dr} + \frac{\varphi_s}{L_s} \end{cases} \tag{18}$$

Regarding reactive and active power, they are related to both rotor current and stator flux, as we find that active power is related to both quadrature rotor current and stator flux. On the other hand, reactive power can be changed by changing both the direct current and the flux. Equation (19) shows both the active and reactive power of the AG [19]:

$$\begin{cases} Q_s = -1.5 \left( \frac{\omega_s \varphi_s M}{L_s} I_{dr} - \frac{\omega_s \varphi_s^2}{L_s} \right) \\ P_s = -1.5 \frac{\omega_s \varphi_s M}{L_s} I_{qr} \end{cases} \tag{19}$$

The torque represented in Equation (12) becomes as follows:

$$T_{em} = -1.5 I_{qr} \cdot \varphi_{ds} \cdot p \cdot \frac{M}{L_s} \tag{20}$$

Direct and quadrature rotor voltages can be expressed by Equation (21). A PI controller is used to give reference values for both direct and quadrature rotor voltages [19]:

$$\begin{cases} V_{dr}^* = K_p \cdot e(t) + K_i \int e(t)dt + g \frac{M \cdot V_s}{L_s} \\ V_{qr}^* = K_p \cdot e(t) + K_i \int e(t)dt - \frac{R_r \cdot \hat{V}_s}{M \cdot \omega_s} \end{cases} \quad (21)$$

where  $V_{dr}^*$  and  $V_{qr}^*$  are the reference direct and quadrature rotor voltages.

In order to give a more illustrative picture of the working principle of the traditional DVC method and to facilitate the understanding of this method, the following figure (Figure 12) shows the working principle of the traditional DVC method.

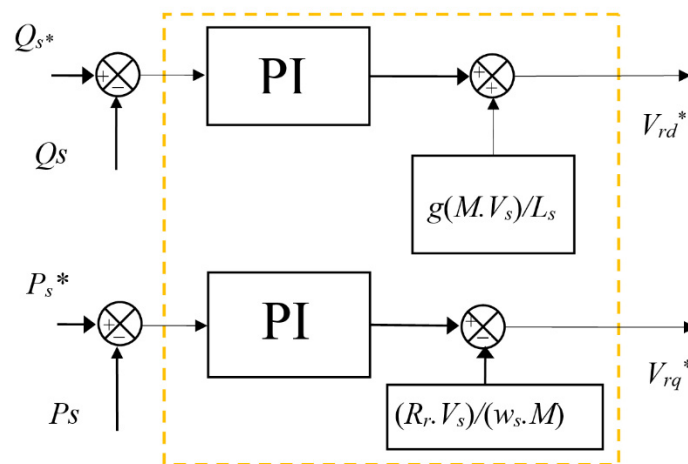


Figure 12. Structure of the traditional DVC method.

This figure was drawn based on Equation (21). The traditional DVC technique is very simple compared to the DTC strategy or to direct power control.

Despite its ease of implementation and simplicity, this traditional DVC technique gives unsatisfactory results or fewer results compared to both the DTC strategy and to the indirect FOC technique. Through the results shown in [19], the classical DVC method gives more fluctuations at the level of current, torque, flux, and reactive power. Moreover, in this method, the THD value of electric current is higher compared to that of the DTC technique, the indirect FOC strategy, and direct power control, and this is because of using both a PI controller and the traditional PWM technique. As it is known, the use of the traditional PWM technique results in an electrical signal with a variable frequency, thus obtaining an unstable speed, and this is a big consequence of using this traditional DVC method. To overcome these obstacles found in the classical DVC method, a new idea for this classical DVC method is proposed, which is shown in the next section.

### 6. Proposed DVC Strategy

In order to ameliorate the performance and effectiveness of the classical DVC technique and to improve the quality of the electric current produced by the asynchronous generator placed in the multi-rotor wind electric power generation system, a new algorithm is given to the classical DVC method, using both the proposed FOPI controller and the proposed IPWM technique, which are used to keep the simplicity and ease of implementing the classical DVC technique. Moreover, the designed DVC technique is a change in the classical DVC method, in which the same shape is maintained with a change in both the traditional PI controller and the PWM technique by replacing them with the proposed FOPI controller and the proposed IPWM technique, respectively. All of this is performed to obtain satisfactory results in a simpler and more durable method. The proposed DVC method based on the FOPI controller using the IPWM technique of the AG integrated into an MRWT system is shown in Figure 13.

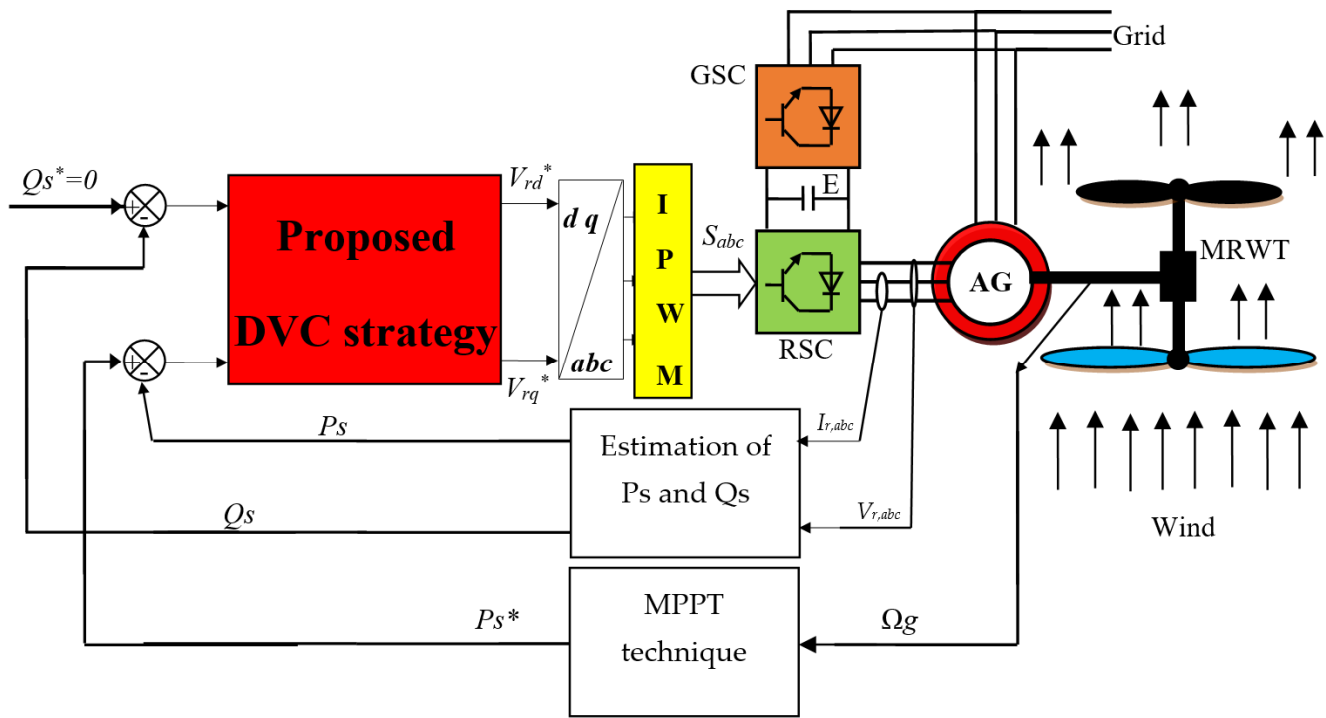


Figure 13. Proposed DVC control of the AG-MRWT system.

In this proposed DVC method, the same level of estimation of both reactive and active power is used in the traditional method. Moreover, the reference value of the reactive power is set to zero, the reference value of the active power is related to the wind speed, and the maximum power point tracking (MPPT) technique is used to obtain the reference value of the active power.

In order to estimate both the reactive power and the active power, we need the stator flux. The latter is related to both current and voltage.

Equations (22) and (23) show how to obtain the stator flux.

$$\begin{cases} \varphi_{s\alpha} = \int_0^t (V_s - R_s i_{s\alpha}) dt \\ \varphi_{s\beta} = \int_0^t (V_s - R_s i_{s\beta}) dt \end{cases} \quad (22)$$

$$|\varphi_s| = \sqrt{(\varphi_{s\beta}^2 + \varphi_{s\alpha}^2)} \quad (23)$$

The reference value for both direct and quadrature rotor voltages using the proposed DVC method is represented by Equation (24):

$$\begin{cases} V_{dr}^* = (K_p \cdot e_d(t) + K_i \int e_d(t) \cdot dt)^\lambda + g \frac{M \cdot V_s}{L_s} \\ V_{qr}^* = (K_p \cdot e_q(t) + K_i \int e_q(t) \cdot dt)^\lambda - \frac{R_r \cdot V_s}{M \cdot \omega_s} \end{cases} \quad (24)$$

where  $\lambda$  is the fractional order ( $\lambda \neq 0$ ), which can take both positive and negative values.

The reference values of both the direct and quadrature rotor voltages are related to the reactive and active power references, respectively.

The errors of the reactive and active power are given by Equation (25):

$$\begin{cases} e_d = Q_s^* - Q_s \\ e_q = P_s^* - P_s \end{cases} \quad (25)$$

If the value of  $\lambda$  is 1, the proposed DVC method becomes the classical DVC method. This is a positive aspect concerning the proposed method, as it is possible to cross from one method to another, and this is performed by changing the value of  $\lambda$  only.

Figure 14 represents the proposed DVC method for improving the performance and effectiveness of the classical DVC method.

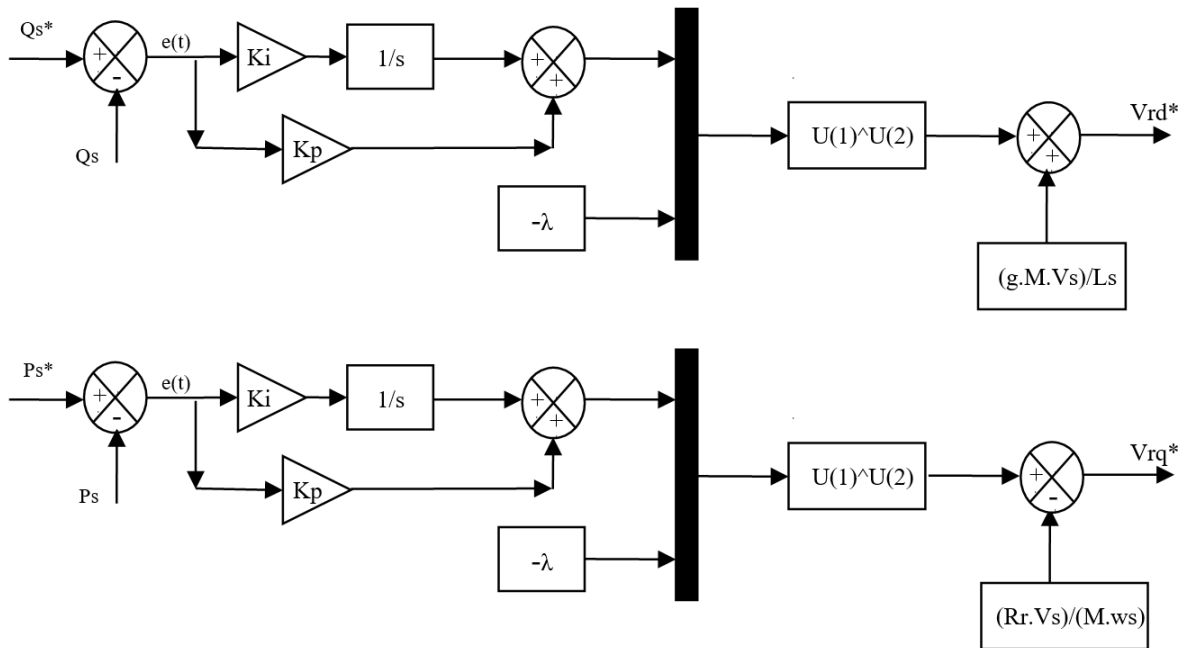


Figure 14. The internal structure of the proposed DVC method.

In Table 2, a comparison is given between the proposed DVC-FOPI using the ANFIS-PWM technique and the traditional DVC strategy. Through this table, the proposed DVC-FOPI using the ANFIS-PWM technique is more robust and reduces power ripples compared to the traditional DVC strategy. In the next section, the results are confirmed, and the robustness of the proposed DVC-FOPI with the ANFIS-PWM technique is verified using the Matlab/Simulink software.

Table 2. A comparative study between the traditional and proposed DVC strategies.

	Conventional DVC Strategy	Proposed DVC Strategy
Type modulation used	PWM	Intelligent PWM
Type controller used	PI controller	FOPI controller
Robustness	Low	High
Rise time	High	Low
Response dynamic	Slow	Quick
Degree of complexity	Low	Low
Ease	Low	Medium
Simplicity of implementation	Low	Low
Power ripple	High	Low
THD	High	Low
Quality of current	Low	High

### 7. Numerical Results

In this part, the designed technique is verified using a simulation in the Matlab program. In this work, the proposed fractional-order DVC (FODVC) strategy based on the ANFIS-PWM strategy (FODVC-ANFIS-PWM) is compared with the classical DVC strategy in terms of THD, ripples of torque, reactive power, current, and active power. A generator with a large amount of power is used to verify the proposed FODVC-ANFIS-PWM method. The generator’s parameters are taken from [7,19]:  $R_s = 0.012 \Omega$ ,  $P_{sn} = 1.5 \text{ MW}$ ,  $380/696 \text{ V}$ ,  $L_r = 0.0136 \text{ H}$ ,  $L_m = 0.0135 \text{ H}$ ,  $J = 1000 \text{ kg}\cdot\text{m}^2$ ,  $R_r = 0.021 \Omega$ ,  $50 \text{ Hz}$ ,  $L_s = 0.0137 \text{ H}$ ,  $p = 2$ , and  $f_r = 0.0024 \text{ Nm/s}$ .

The robustness of the proposed FODVC-ANFIS-PWM method of the asynchronous generator integrated into an MRWT system is verified by using two tests, and this is always in comparison with the classical DVC method. The first test is used to study the behavior of the follower of the references, and the second test is used to study the change in the behavior of the proposed FODVC-ANFIS-PWM method in the event of a change in the generator's parameters.

#### A. First test

The results of this test are shown in Figure 15. Figure 15 represents current, reactive power, torque, and active power. In this figure, we find that the designed FODVC-ANFIS-PWM technique gives good results in terms of dynamic response. In addition, reactive and active power follow the references well, and this is for both the proposed and the traditional DVC method (see Figure 15a,b). The active power changes according to the change in wind speed, by which we find that the greater that the wind speed is, the greater that the value of the active power is, and vice versa. The proposed FODVC-ANFIS-PWM technique gives satisfactory results in terms of its dynamic response to active power compared to the classical DVC strategy. Regarding the reactive power, it is zero, with the presence of ripples. Through these results, the proposed FODVC-ANFIS-PWM technique has a much better dynamic response to reactive power than the traditional DVC technique.

Figure 15c represents the torque of both strategies, and it takes the form of active power, as its value is affected by wind speed. Moreover, torque is related to active power, and its value increases as the value of the active power increases, as we find the value of the torque ranging between 0 Nm and  $-9000$  Nm. Concerning the current, it is shown in Figure 15d, where it is a sinusoidal current and where it is also related to wind speed. The change in current is related to the change in wind speed. Moreover, the current takes the form of active power, and its value increases as the value of the active power increases. We find that the largest value of the current is about 3000 A, and the lowest value is about 3000 A.

Figure 15e,f show the THD value of the stator current of both techniques. In Figure 15e,f, it can be observed that the THD value is reduced for the proposed FODVC-ANFIS-PWM technique (0.10%) in comparison to the DVC technique (1.18%). The proposed FODVC-ANFIS-PWM technique minimizes the THD value of stator current by about 91.52%.

Figure 16 represents the ripples of the reactive power, torque, active power, and stator current of the traditional and proposed FODVC-ANFIS-PWM strategies. In this figure, the proposed FODVC-ANFIS-PWM strategy minimizes the ripples in the torque, reactive power, stator current, and reactive power in comparison to the classical DVC strategy.

#### B. Robustness test

In this test, the values of  $R_s$ ,  $L_s$ ,  $M$ ,  $L_r$ , and  $R_r$  are changed to new values in order to study the behavior of the proposed method compared with the classical method. Moreover, this is performed in order to know the extent to which the proposed method is affected compared to the classical DVC technique in case the parameters of the studied system change. In this test, the values of  $L_s$ ,  $L_r$ ,  $R_s$ ,  $L_m$ , and  $R_r$  become 0.00685 H, 0.0068 H, 0.024  $\Omega$ , 0.00675 H, and 0.042  $\Omega$ , respectively. The results obtained are illustrated in Figure 17a–f. Figure 17 represents the current, reactive power, torque, and active power of the proposed and traditional techniques. In these figures, the reactive power and the active power follow the references well, with a preference for the proposed FODVC-ANFIS-PWM method in the aspect of the speed of response time (see Figure 17a,b).

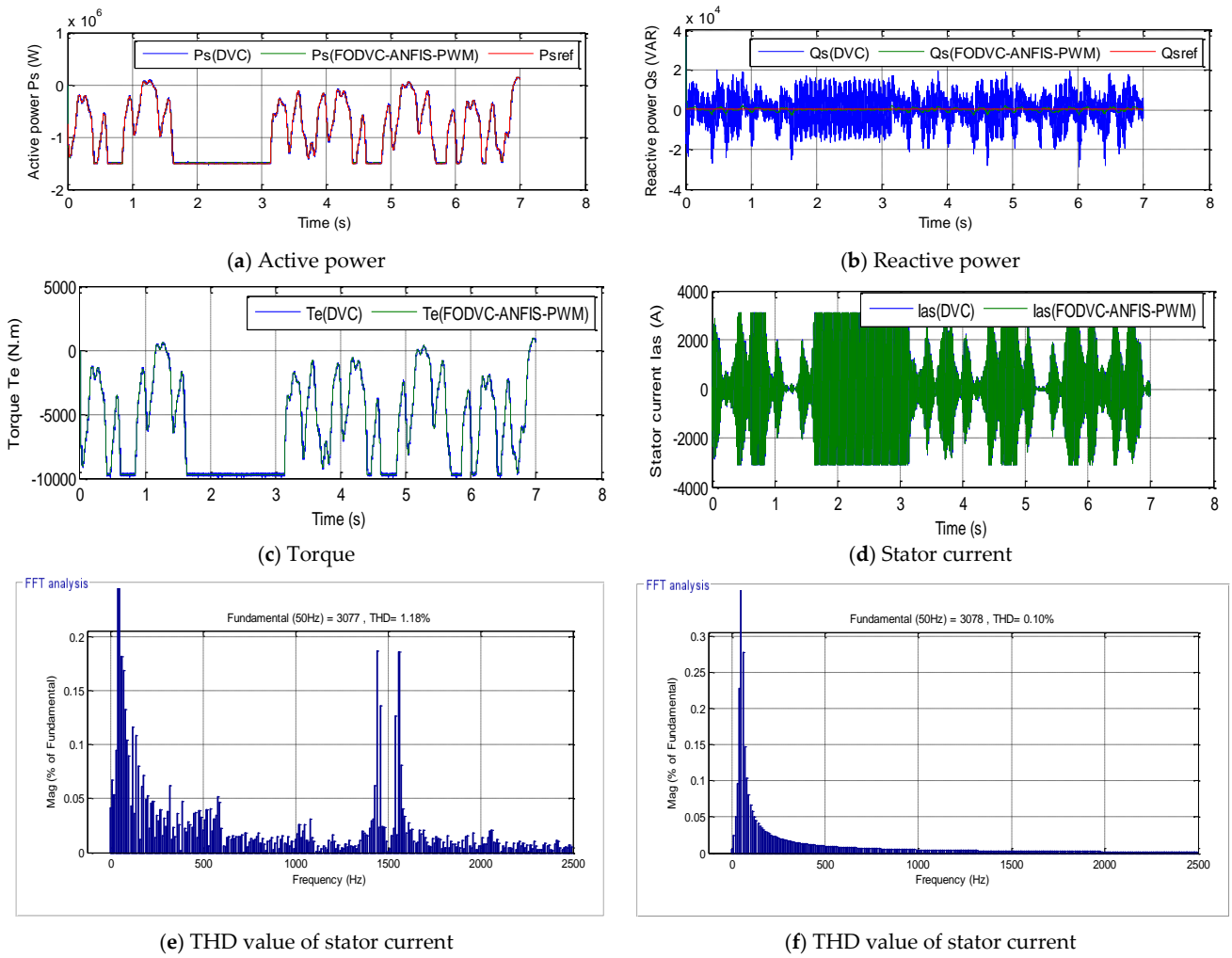


Figure 15. Simulated results from the first test.

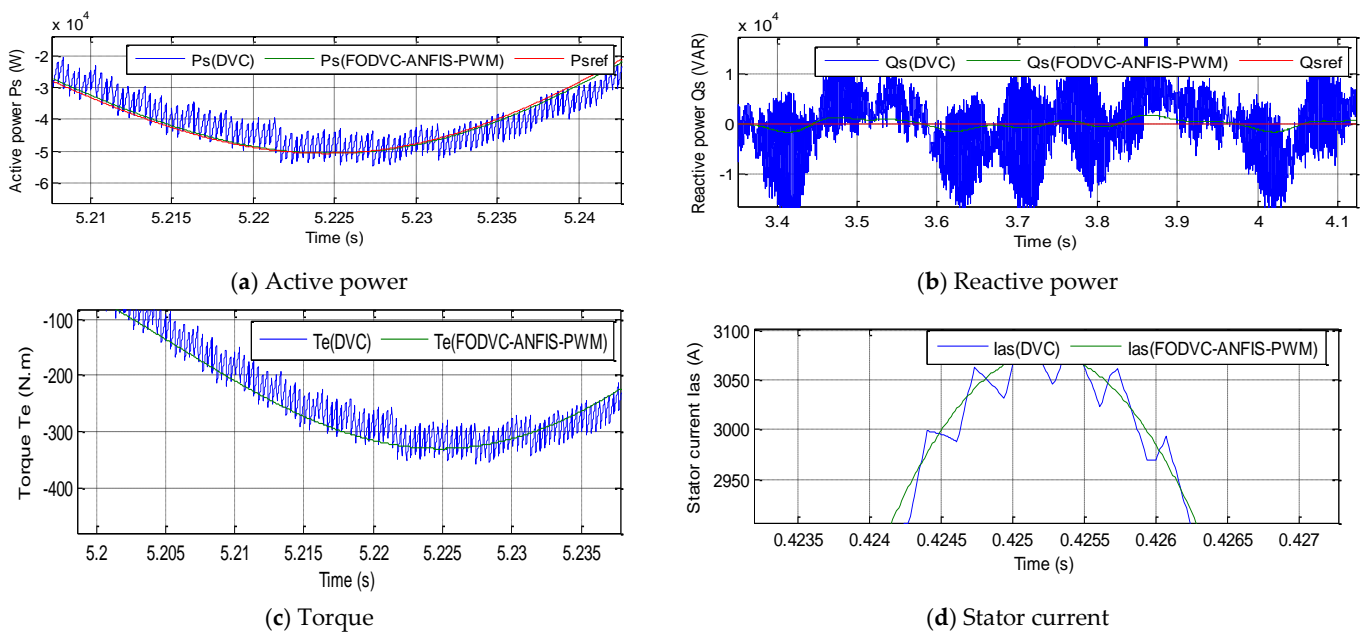


Figure 16. Zoom in the reactive power, torque, active power, and current.

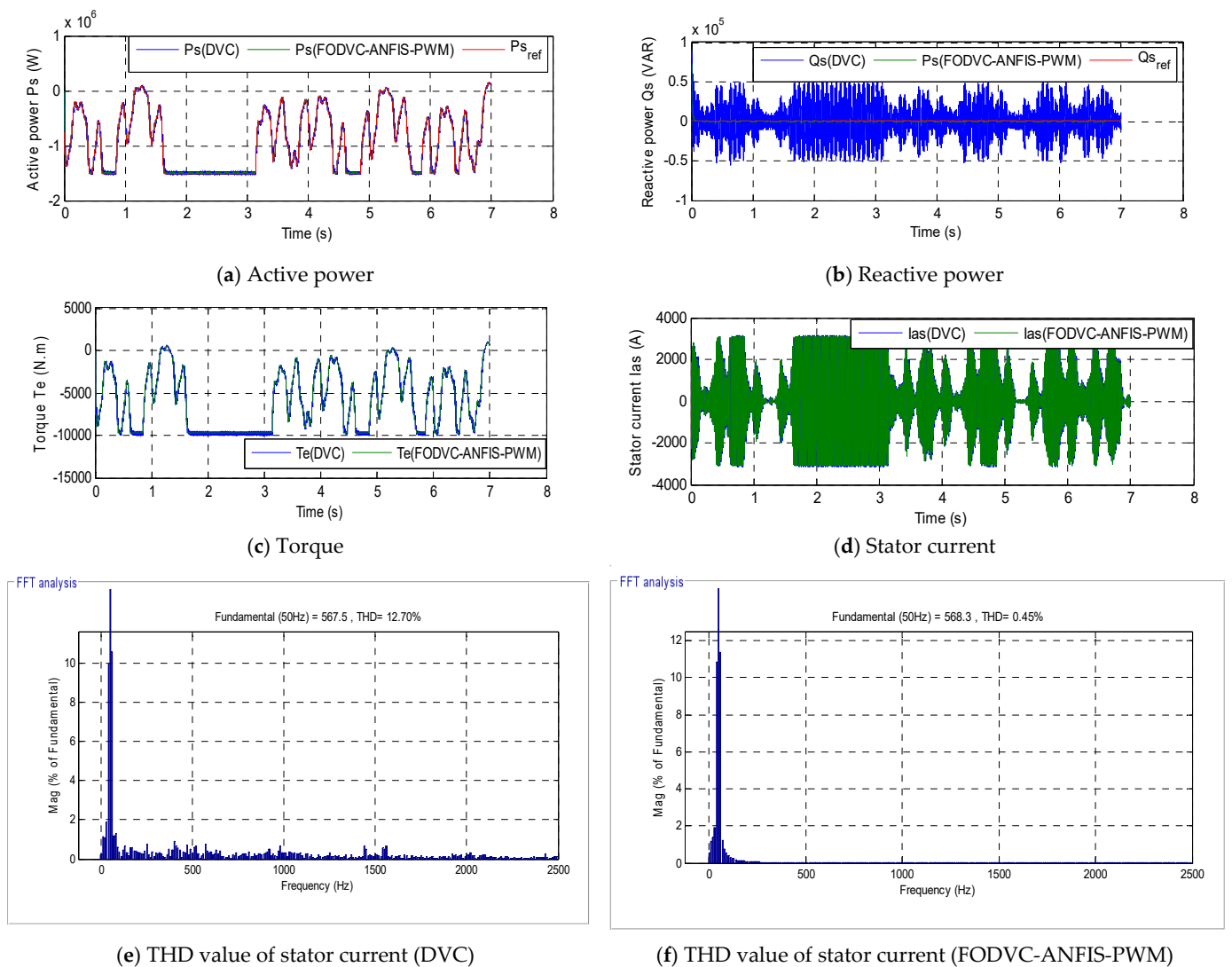


Figure 17. Simulated results from the second test.

The current and torque are represented in Figure 17c,d, and each of them takes the same form as the active power, for which the greater that the value of the active power is, the greater that the values of both current and torque are. The maximum torque is 100 Nm, and the minimum value is  $-10,000$  Nm for both DVC methods. The proposed FODVC-ANFIS-PWM method in this test gives an excellent value of THD (0.45%) compared to the DVC method (12.47%), and the reduction ratio is about 96.45%. Despite a change in some parameters of the generator, the proposed FODVC-ANFIS-PWM technique gives excellent results in terms of the value of the ripples' amplitude of torque, current, reactive power, and active power compared to those of the traditional DVC method (See Figure 18a–f).

The results obtained from the two tests are shown in Table 3. In this table, the designed FODVC-ANFIS-PWM technique gives excellent results in terms of reducing the ripples of reactive power, torque, active power, and current, and this indicates the robustness of the designed strategy. Moreover, the proposed FODVC-ANFIS-PWM technique minimizes the active power ripple's amplitude compared to the DVC method by about 99.99% and 99.96% in the first and second tests, respectively. Regarding the reactive power, the percentages are 99.93% and 99.97% in the first and second tests, respectively.

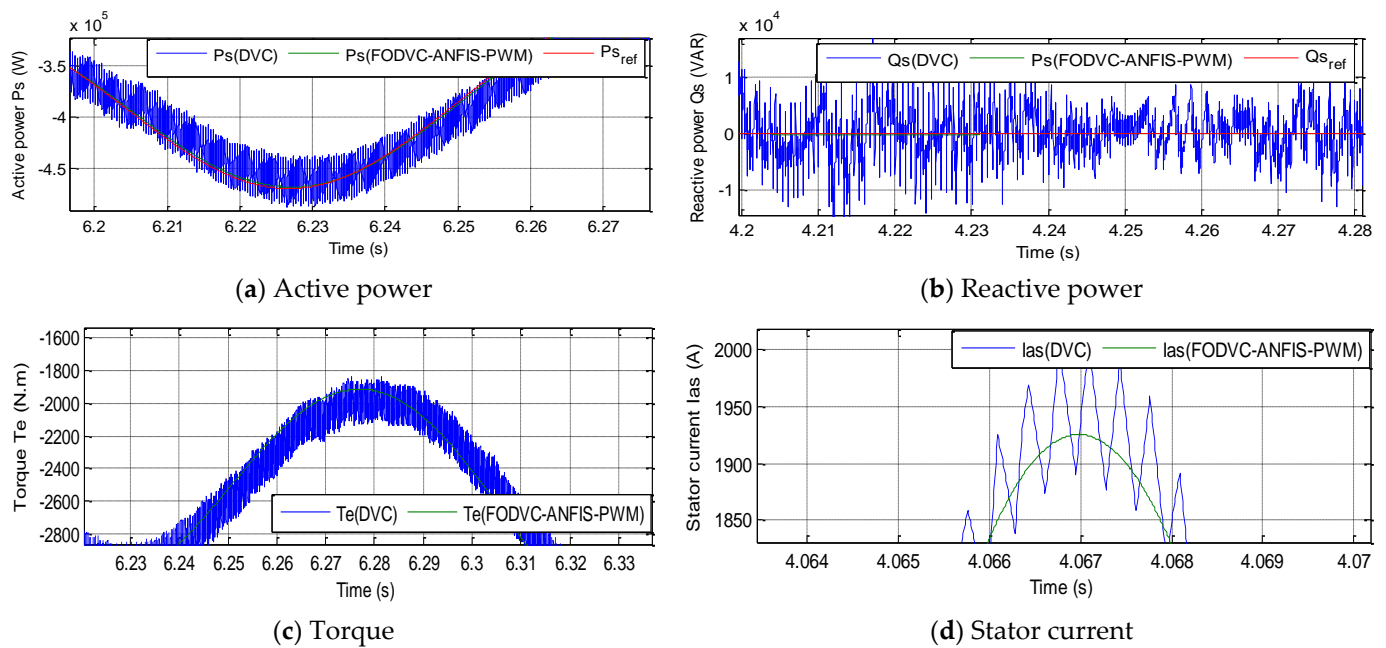


Figure 18. Zoom in the reactive power, active power, torque, and current.

Table 3. A comparative study between the two techniques.

		Reactive Power (VAR)	Torque (Nm)	Current (A)	Active Power (W)
DVC strategy	First test	60,000	150	100	30,000
	Second test	309,000	800	200	100,000
FODVC-ANFIS-PWM strategy	First test	40	10	15	10
	Second test	80	20	20	40
Ratios	First test	99.93%	93.33%	85%	99.99%
	Second test	99.97%	97.50%	90%	99.96%

In the case of electromagnetic torque, the reduction rates are 93.33% and 97.50% in the first and second tests, respectively. The same applies to the stator current. The proposed FODVC-ANFIS-PWM method provides excellent ratios in the case of the two tests compared to the DVC strategy.

The proposed FOPI controller allows for smoother control of active and reactive power, and it minimizes the ripples of the torque, active power, and current of the AG-based MRWT system. The results show a significant reduction in electric current ripples and an improvement in the quality of the energy produced. It has already been shown that the FOPI controller is superior to the PI controller during sudden changes in wind speed, and this is in the case of either changing or not changing the parameters of the generator. In this paper, the RSC control method is implemented separately using the PI and proposed FOPI controller to compare their performances in the case of variable wind speed. The simulation results are shown in Figures 15 and 17 and in Table 3. The results show that, using a proposed FOPI controller, the amplitude of the ripples of torque, current, and active power is reduced. Therefore, the proposed FOPI controller has better performance and is more efficient in DFIG power control compared to other consoles. This indicates the robustness of the designed FODVC-ANFIS-PWM strategy in improving the quality of active power and electric current.

In Table 4, the THD ratio of the electric current of the asynchronous generator obtained by the proposed FODVC-ANFIS-PWM method is compared with that obtained in some papers published in the most prestigious scientific journals. In this table, the designed FODVC-ANFIS-PWM technique provides a better THD value than several techniques, such as DTC, DPC, and indirect field-oriented control.

**Table 4.** A comparative study between the designed FODVC-ANFIS-PWM strategy and other works in terms of the value of THD.

	Techniques	THD (%)	
Ref. [58]	Direct torque control	2.57	
Ref. [59]	Power control	Strategy 1	5.6817
		Strategy 2	3.1873
Ref. [60]	Field-oriented control	3.7	
Ref. [61]	Classical direct torque control	6.70	
	Fuzzy direct torque control	2.40	
Ref. [62]	Direct power control with IP controllers	0.43	
Ref. [63]	Indirect field-oriented control	6.5	
Ref. [64]	12 sectors direct power control	0.40	
Ref. [65]	Fuzzy sliding mode control	1.15	
Ref. [66]	Direct torque control	7.83	
	Neural direct torque control	3.26	
Ref. [22]	Second-order sliding mode control	3.13	
Ref. [67]	DTC technique using L-filter	10.79	
	DPC strategy using LCL-filter	4.05	
Ref. [68]	DPC strategy with STA controller	1.66	
Ref. [23]	DVC with synergetic sliding mode controller	0.50	
Ref. [69]	Integral sliding mode control	9.71	
	Multi-resonant-based sliding mode controller	3.14	
Ref. [70]	Two-level direct torque control	8.75	
	Three-level direct torque control	1.57	
Ref. [71]	Genetic Algorithm Least Squares Wavelet Support Vector Machines (GA-LS-WSVM) method	3.39	
Designed FODVC-ANFIS-PWM technique	First test	0.10	
	Second test	0.45	

## 8. Conclusions

In this work, an electric power generation system using multi-rotor wind energy is presented, in which an asynchronous generator is used to generate electric current due to its durability. In order to control the generator, a new, more robust direct vector control strategy is proposed based on the use of both the proposed FOPI controller and the designed intelligent PWM technique. The proposed FODVC-ANFIS-PWM technique is compared with the classical DVC technique, and the designed FODVC-ANFIS-PWM technique is implemented in the Matlab program. The simulation results show the characteristics of the designed FODVC-ANFIS-PWM technique in the case of changing the generator's parameters and in the case of changing wind speed. The proposed FODVC-ANFIS-PWM method reduces the ripples of active power, torque, current, and reactive power compared to the classical DVC method. Moreover, the THD ratio of the current is reduced compared to the DVC technique.

The results obtained from this work can be summarized in the following points:

- A new fractional-order PI controller is presented and applied to the DVC strategy.
- A novel PWM strategy based on an ANFIS algorithm was presented to control the inverter of the generator to reduce torque, active power, current, and reactive power ripples.

- A robust strategy is proposed that reduces the THD value of the current.
- A new robust control strategy is proposed and presented.

In future work, a new way to control an asynchronous generator by integrating between nonlinear methods and artificial intelligence methods, such as the PSO algorithm and genetic algorithm, can be tested. Additionally, experimental testing of the method proposed in this paper can be considered.

**Author Contributions:** Validation: N.B., P.T. and N.T.; Conceptualization: H.B.; Software: H.B.; Methodology: H.B.; Investigation: H.B.; Resources: H.B., N.B., P.T. and N.T.; Project administration: N.B.; Data Curation: N.B., P.T. and N.T.; Writing—Original Draft Preparation: H.B.; Supervision: N.B. and I.C.; Visualization: I.C. and N.B.; Formal analysis: N.B.; Funding acquisition: N.B., P.T. and N.T.; Writing—Review and Editing: I.C., N.B., P.T., N.T. and H.B. All authors have read and agreed to the published version of the manuscript.

**Funding:** This work was supported in part by the Framework Agreement between the University of Pitesti (Romania) and King Mongkut's University of Technology, North Bangkok (Thailand); in part by an International Research Partnership, "Electrical Engineering—Thai French Research Center (EE-TFRC)", under the project framework of the Lorraine Université d'Excellence (LUE) in cooperation between Université de Lorraine and King Mongkut's University of Technology, North Bangkok; in part by the National Research Council of Thailand (NRCT) under the Senior Research Scholar Program under Grant No. N42A640328; and in part by the National Science, Research, and Innovation Fund (NSRF) under King Mongkut's University of Technology, North Bangkok, under Grant no. KMUTNB-FF-65-20.

**Institutional Review Board Statement:** Not applicable.

**Informed Consent Statement:** Not applicable.

**Data Availability Statement:** Not applicable.

**Conflicts of Interest:** The authors declare no conflict of interest.

## References

1. Abdelrahem, M.; Hackl, C.M.; Kennel, R. Limited-Position Set Model-Reference Adaptive Observer for Control of DFIGs without Mechanical Sensors. *Machines* **2020**, *8*, 72. [CrossRef]
2. Nnem, L.M.; Lonla, B.M.; Sonfack, G.B.; Mbih, J. Review of a Multipurpose Duty-Cycle Modulation Technology in Electrical and Electronics Engineering. *J. Electr. Eng. Electron. Control. Comput. Sci.* **2018**, *4*, 9–18. Available online: <https://jeeccs.net/index.php/journal/article/view/101> (accessed on 19 April 2022).
3. Alhato, M.M.; Ibrahim, M.N.; Rezk, H.; Bouallègue, S. An Enhanced DC-Link Voltage Response for Wind-Driven Doubly Fed Induction Generator Using Adaptive Fuzzy Extended State Observer and Sliding Mode Control. *Mathematics* **2021**, *9*, 963. [CrossRef]
4. Habib, B.; Boudjema, Z.; Belaidi, A. Higher control scheme using neural second order sliding mode and ANFIS-SVM strategy for a DFIG-based wind turbine. *Int. J. Adv. Telecommun. Electrotech. Signals Syst.* **2019**, *8*, 17–28.
5. Giaourakis, D.G.; Safacas, A.N. Effect of Short-Circuit Faults in the Back-to-Back Power Electronic Converter and Rotor Terminals on the Operational Behavior of the Doubly-Fed Induction Generator Wind Energy Conversion System. *Machines* **2015**, *3*, 2–26. [CrossRef]
6. Mohan Kumar, P.; Sivalingam, K.; Lim, T.-C.; Ramakrishna, S.; Wei, H. Strategies for Enhancing the Low Wind Speed Performance of H-Darrieus Wind Turbine-Part 1. *Clean Technol.* **2019**, *1*, 185–204. [CrossRef]
7. Benbouhenni, H.; Bizon, N. Improved Rotor Flux and Torque Control Based on the Third-Order Sliding Mode Scheme Applied to the Asynchronous Generator for the Single-Rotor Wind Turbine. *Mathematics* **2021**, *9*, 2297. [CrossRef]
8. Ullah, W.; Khan, F.; Hussain, S. A Novel Dual Rotor Permanent Magnet Flux Switching Generator for Counter Rotating Wind Turbine Applications. *IEEE Access* **2022**, *10*, 16456–16467. [CrossRef]
9. Yahdou, A.; Djilali, A.B.; Boudjema, Z.; Mehedi, F. Improved Vector Control of a Counter-Rotating Wind Turbine System Using Adaptive Backstepping Sliding Mode. *J. Eur. Systèmes Autom.* **2020**, *53*, 645–651. [CrossRef]
10. Luo, X.; Niu, S. A Novel Contra-Rotating Power Split Transmission System for Wind Power Generation and Its Dual MPPT Control Strategy. *IEEE Trans. Power Electron.* **2017**, *32*, 6924–6935. [CrossRef]
11. Onyishi, D.U.; Ofualagba, G. Analysis of the Electricity Distribution Supply in Eastern Nigeria: Current Challenges and Possible Solutions. *J. Electr. Eng. Electron. Control. Comput. Sci.* **2021**, *7*, 1–8. Available online: <https://jeeccs.net/index.php/journal/article/view/209> (accessed on 19 April 2022).

12. Shahzad, U. Application of Machine Learning for Optimal Wind Farm Location. *J. Electr. Eng. Electron. Control. Comput. Sci.* **2022**, *8*, 1–8. Available online: <https://jeeeccs.net/index.php/journal/article/view/276> (accessed on 19 April 2022).
13. Zhao, W.; Lipo, T.A.; Kwon, B.-I. A novel dual-rotor axial field fault-tolerant flux-switching permanent magnet machine with high-torque performance. *IEEE Trans. Magn.* **2015**, *51*, 1–4. [[CrossRef](#)]
14. No, T.S.; Kim, J.-K.; Moon, J.H.; Kim, S.J. Modeling control and simulation of dual rotor wind turbine generator system. *Renew. Energy* **2009**, *34*, 2124–2132. [[CrossRef](#)]
15. Kumar, P.S.; Abraham, A.; Bensingh, R.J.; Ilangoan, S. Computational and experimental analysis of a counter-rotating wind turbine system. *J. Sci. Ind. Res.* **2013**, *72*, 300–306.
16. Giger, U.; Kleinhansl, S.; Schulte, H. Design Study of Multi-Rotor and Multi-Generator Wind Turbine with Lattice Tower—A Mechatronic Approach. *Appl. Sci.* **2021**, *11*, 11043. [[CrossRef](#)]
17. Salic, T.; Charpentier, J.F.; Benbouzid, M.; Le Boulluec, M. Control Strategies for Floating Offshore Wind Turbine: Challenges and Trends. *Electronics* **2019**, *8*, 1185. [[CrossRef](#)]
18. Velpula, S.; Thirumalaivasan, R.; Janaki, M. Stability Analysis on Torsional Interactions of Turbine-Generator Connected with DFIG-WECS Using Admittance Model. *IEEE Trans. Power Syst.* **2020**, *35*, 4745–4755. [[CrossRef](#)]
19. Benbouhenni, H.; Bizon, N. Terminal Synergetic Control for Direct Active and Reactive Powers in Asynchronous Generator-Based Dual-Rotor Wind Power Systems. *Electronics* **2021**, *10*, 1880. [[CrossRef](#)]
20. Benbouhenni, H.; Bizon, N. Third-Order Sliding Mode Applied to the Direct Field-Oriented Control of the Asynchronous Generator for Variable-Speed Contra-Rotating Wind Turbine Generation Systems. *Energies* **2021**, *14*, 5877. [[CrossRef](#)]
21. Habib, B. Amelioration effectiveness of torque and rotor flux control applied to the asynchronous generator (AG) for dual-rotor wind turbine using neural third-order sliding mode approaches. *Int. J. Eng. Trans. C Asp.* **2022**, *35*, 517–530.
22. Yahdou, A.; Hemici, B.; Boudjema, Z. Second order sliding mode control of a dual-rotor wind turbine system by employing a matrix converter. *J. Electr. Eng.* **2016**, *16*, 1–11.
23. Benbouhenni, H.; Bizon, N. A Synergetic Sliding Mode Controller Applied to Direct Field-Oriented Control of Induction Generator-Based Variable Speed Dual-Rotor Wind Turbines. *Energies* **2021**, *14*, 4437. [[CrossRef](#)]
24. Habib, B. Synergetic control theory scheme for asynchronous generator based dual-rotor wind power. *J. Electr. Eng. Electron. Control Comput. Sci.* **2021**, *7*, 19–28. Available online: <https://jeeeccs.net/index.php/journal/article/view/215> (accessed on 9 April 2022).
25. Sami, I.; Ullah, S.; Ali, Z.; Ullah, N.; Ro, J.-S. A Super Twisting Fractional Order Terminal Sliding Mode Control for DFIG-Based Wind Energy Conversion System. *Energies* **2020**, *13*, 2158. [[CrossRef](#)]
26. Almakki, A.N.J.; Andrey, A.M. Application of fractional-order second-order continuous sliding mode controller in direct flux and torque control system of doubly-fed induction generator integrated to wind turbine: Simulation studies. *Vestn. Gos. Univ. Morskogo I Rechn. Flot. Im. Admirala S. O. Makarova* **2021**, *13*, 887–907. [[CrossRef](#)]
27. Heydari, E.E.; Rafiee, M.; Pichan, M. Fuzzy-Genetic Algorithm-Based Direct Power Control Strategy for DFIG. *Iran. J. Electr. Electron. Eng.* **2018**, *14*, 353–361. [[CrossRef](#)]
28. Xu, S.; Sun, H.; Zhang, Z.; Guo, Q.; Zhao, B.; Bi, J.; Zhang, B. MAS-Based Decentralized Coordinated Control Strategy in a Micro-Grid with Multiple Microsources. *Energies* **2020**, *13*, 2141. [[CrossRef](#)]
29. Mehdi, H.; Farzad, R.S. Analysis and detection of a wind system failure in a micro-grid. *J. Renew. Sustain. Energy* **2016**, *8*, 043302. [[CrossRef](#)]
30. Chen, H.; Chen, X.; Xie, W. Fractional-Order PI Controller for DFIG-Based Marine Tidal Current Applications. In Proceedings of the 2018 IEEE International Power Electronics and Application Conference and Exposition (PEAC), Shenzhen, China, 4–7 November 2018; pp. 1–6. [[CrossRef](#)]
31. Zhibin, Z.; Hao, C.; Wei, X.; Xiyang, C.; Jingang, H.; Nadia, A.; Tianhao, T.; Mohamed, B. Fractional-Order PI Control of DFIG-Based Tidal Stream Turbine. *J. Mar. Sci. Eng.* **2020**, *8*, 309. [[CrossRef](#)]
32. Mosaad, M.I.; Abu-Siada, A.; El-Naggar, M.F. Application of Superconductors to Improve the Performance of DFIG-Based WECS. *IEEE Access* **2019**, *7*, 103760–103769. [[CrossRef](#)]
33. Hossein, M.; Seyed, A.T.; Mohsen, R.; Mohammad, S. DFIG performance improvement in grid connected mode by using fractional order [PI] controller. *Int. J. Electr. Power Energy Syst.* **2018**, *96*, 398–411. [[CrossRef](#)]
34. Beik, O.; Al-Adsani, A.S. Active and Passive Control of a Dual Rotor Wind Turbine Generator for DC Grids. *IEEE Access* **2021**, *9*, 1987–1995. [[CrossRef](#)]
35. Wang, B.; Wang, S.; Peng, Y.; Pi, Y.; Luo, Y. Design and High-Order Precision Numerical Implementation of Fractional-Order PI Controller for PMSM Speed System Based on FPGA. *Fractal Fract.* **2022**, *6*, 218. [[CrossRef](#)]
36. Zheng, J.; Jiang, X.; Ren, G.; Xie, X.; Fan, D. High-Precision Anti-Interference Control of Direct Drive Components. *Actuators* **2022**, *11*, 95. [[CrossRef](#)]
37. Li, G.; Li, Y.; Chen, H.; Deng, W. Fractional-Order Controller for Course-Keeping of Under actuated Surface Vessels Based on Frequency Domain Specification and Improved Particle Swarm Optimization Algorithm. *Appl. Sci.* **2022**, *12*, 3139. [[CrossRef](#)]
38. Vu, T.N.L.; Chuong, V.L.; Truong, N.T.N.; Jung, J.H. Analytical Design of Fractional-Order PI Controller for Parallel Cascade Control Systems. *Appl. Sci.* **2022**, *12*, 2222. [[CrossRef](#)]
39. Nikkhah Kashani, H.; Rouhi Ardeshiri, R.; Gheisarnejad, M.; Khooban, M.-H. Optimal Cascade Non-Integer Controller for Shunt Active Power Filter: Real-Time Implementation. *Designs* **2022**, *6*, 32. [[CrossRef](#)]

40. Rostami, M.; Madani, S.M.; Ademi, S. Sensorless Closed-Loop Voltage and Frequency Control of Stand-Alone DFIGs Introducing Direct Flux-Vector Control. *IEEE Trans. Ind. Electron.* **2020**, *67*, 6078–6088. [CrossRef]
41. Erturk, E.; Sivrioglu, S.; Bolat, F.C. Analysis Model of a Small Scale Counter-Rotating Dual Rotor Wind Turbine with Double Rotational Generator Armature. *Int. J. Renew. Energy Res.* **2018**, *8*, 1849–1858.
42. Fukami, T.; Momiyama, M.; Shima, K.; Hanaoka, R.; Takata, S. Steady-State Analysis of a Dual-Winding Reluctance Generator with a Multiple-Barrier Rotor. *IEEE Trans. Energy Convers.* **2008**, *23*, 492–498. [CrossRef]
43. Tejado, I.; Vinagre, B.M.; Traver, J.E.; Prieto-Arranz, J.; Nuevo-Gallardo, C. Back to Basics: Meaning of the Parameters of Fractional Order PID Controllers. *Mathematics* **2019**, *7*, 530. [CrossRef]
44. Muresan, C.I.; Birs, I.R.; Dulf, E.H. Event-Based Implementation of Fractional Order IMC Controllers for Simple FOPDT Processes. *Mathematics* **2020**, *8*, 1378. [CrossRef]
45. Mohamed Ahmed, S.A.; Montaser Abd El Sattar, M.A. Dynamic Performance and Effectiveness of Voltage Disturbances on the Improvement of Power Quality for Grid-Connected DFIG System Based Wind Farm. *J. Electr. Eng. Electron. Control. Comput. Sci.* **2020**, *5*, 25–30. Available online: <https://jeeeccs.net/index.php/journal/article/view/126> (accessed on 19 April 2022).
46. Yingjie, W.; Hui, Z.; Hao, L.; Bowei, P. Dynamic Analysis of Grid-Connected DFIG with Fractional-Order PI Control. In Proceedings of the 2019 14th IEEE Conference on Industrial Electronics and Applications (ICIEA), Xi'an, China, 19–21 June 2019; pp. 1690–1693. [CrossRef]
47. Meraj, M.; Rahman, S.; Iqbal, A.; Al Emadi, N. Novel Level Shifted PWM Technique for Unequal and Equal Power Sharing in Quasi Z-Source Cascaded Multilevel Inverter for PV Systems. *IEEE J. Emerg. Sel. Top. Power Electron.* **2021**, *9*, 937–948. [CrossRef]
48. Lee, S.S.; Siwakoti, Y.P.; Lim, C.S.; Lee, K.-B. An Improved PWM Technique to Achieve Continuous Input Current in Common-Ground Transformer less Boost Inverter. *IEEE Trans. Circuits Syst. II Express Briefs* **2020**, *67*, 3133–3136. [CrossRef]
49. Bogaraj, T.; Kanakaraj, J. A Novel Energy Management Scheme using ANFIS for Independent Microgrid. *Int. J. Renew. Energy Res.* **2016**, *6*, 735–746.
50. Fekry, H.M.; Eldesouky, A.A.; Kassem, A.M.; Abdelaziz, A.Y. Power Management Strategy Based on Adaptive Neuro Fuzzy Inference System for AC Microgrid. *IEEE Access* **2020**, *8*, 192087–192100. [CrossRef]
51. Nicola, M.; Nicola, C.-I. Sensorless Fractional Order Control of PMSM Based on Synergetic and Sliding Mode Controllers. *Electronics* **2020**, *9*, 1494. [CrossRef]
52. Bauer, W.; Baranowski, J. Fractional PIAD Controller Design for a Magnetic Levitation System. *Electronics* **2020**, *9*, 2135. [CrossRef]
53. Alam, M.S.; Al-Ismail, F.S.; Abido, M.A. PV/Wind-Integrated Low-Inertia System Frequency Control: PSO-Optimized Fractional-Order PI-Based SMES Approach. *Sustainability* **2021**, *13*, 7622. [CrossRef]
54. Reddy, C.R.; Goud, B.S.; Aymen, F.; Rao, G.S.; Bortoni, E.C. Power Quality Improvement in HRES Grid Connected System with FOPID Based Atom Search Optimization Technique. *Energies* **2021**, *14*, 5812. [CrossRef]
55. Azab, M.; Serrano-Fontova, A. Optimal Tuning of Fractional Order Controllers for Dual Active Bridge-Based DC Microgrid Including Voltage Stability Assessment. *Electronics* **2021**, *10*, 1109. [CrossRef]
56. Ding, J.; Jiao, X. A Novel Control Method of Clutch During Mode Transition of Single-Shaft Parallel Hybrid Electric Vehicles. *Electronics* **2020**, *9*, 54. [CrossRef]
57. Benbouhenni, H.; Bizon, N. Advanced Direct Vector Control Method for Optimizing the Operation of a Double-Powered Induction Generator-Based Dual-Rotor Wind Turbine System. *Mathematics* **2021**, *9*, 2403. [CrossRef]
58. Boudjema, Z.; Taleb, R.; Djerriri, Y.; Yahdou, A. A novel direct torque control using second order continuous sliding mode of a doubly fed induction generator for a wind energy conversion system. *Turk. J. Electr. Eng. Comput. Sci.* **2017**, *25*, 965–975. [CrossRef]
59. Moreira, A.B.; Barros, T.A.D.S.; Teixeira, V.S.D.C.; Souza, R.R.D.; Paula, M.V.D.; Filho, E.R. Control of Powers for Wind Power Generation and Grid Current Harmonics Filtering from Doubly Fed Induction Generator: Comparison of Two Strategies. *IEEE Access* **2019**, *7*, 32703–32713. [CrossRef]
60. Amrane, F.; Chaiba, A.; Babas, B.E.; Mekhilef, S. Design and implementation of high performance field oriented control for grid-connected doubly fed induction generator via hysteresis rotor current controller. *Rev. Sci. Technol.-Electrotechn. Energ.* **2016**, *61*, 319–324.
61. Ayrira, W.; Ourahoua, M.; El Hassounia, B.; Haddib, A. Direct torque control improvement of a variable speed DFIG based on a fuzzy inference system. *Math. Comput. Simul.* **2020**, *167*, 308–324. [CrossRef]
62. Fayssal, A.; Bruno, F.; Azeddine, C. Experimental investigation of efficient and simple wind-turbine based on DFIG-direct power control using LCL-filter for stand-alone mode. *ISA Trans.* **2021**; 1–34, in press. [CrossRef]
63. Sara, M.; Ahmed, E.; Issam, M.; Tamou, N.; Badre, B.I.; Ben Tarla, L. Performance of a vector control for DFIG driven by wind turbine: Real time simulation using DS1104 controller board. *Int. J. Power Electron. Drive Syst.* **2019**, *10*, 1003–1013. [CrossRef]
64. Yusoff, N.A.; Razali, A.M.; Karim, K.A.; Sutikno, T.; Jidin, A. A concept of virtual-flux direct power control of three-phase AC-DC converter. *Int. J. Power Electron. Drive Syst.* **2017**, *8*, 1776–1784. [CrossRef]
65. Boudjema, Z.; Meroufel, A.; Djerriri, Y.; Bounadja, E. Fuzzy sliding mode control of a doubly fed induction generator for energy conversion. *Carpathian J. Electron. Comput. Eng.* **2013**, *6*, 7–14.
66. Said, M.; Derouich, A.; El Ouanjli, N.; El Mahfoud, M. Enhancement of the Direct Torque Control by using Artificial Neuron Network for a Doubly Fed Induction Motor. *Intell. Syst. Appl.* **2022**, *13*, 200060. [CrossRef]

67. Alhato, M.M.; Bouallègue, S. Direct Power Control Optimization for Doubly Fed Induction Generator Based Wind Turbine Systems. *Math. Comput. Appl.* **2019**, *24*, 77. [[CrossRef](#)]
68. Yaichi, I.; Semmah, A.; Wira, P.; Djeriri, Y. Super-twisting sliding mode control of a doubly-fed induction generator based on the SVM strategy. *Period. Polytech. Electr. Eng. Comput. Sci.* **2019**, *63*, 178–190. [[CrossRef](#)]
69. Quan, Y.; Hang, L.; He, Y.; Zhang, Y. Multi-Resonant-Based Sliding Mode Control of DFIG-Based Wind System under Unbalanced and Harmonic Network Conditions. *Appl. Sci.* **2019**, *9*, 1124. [[CrossRef](#)]
70. El Ouanjli, N.; Aziz, D.; El Ghzizal, A.; Mohammed, T.; Youness, E.; Khalid, M.; Badre, B. Direct torque control of doubly fed induction motor using three-level NPC inverter. *Prot. Control. Mod. Power Syst.* **2019**, *4*, 1–9. [[CrossRef](#)]
71. Kamarzarrin, M.; Refan, M.H.; Amiri, P.; Dameshghi, A. Fault Diagnosis of Wind Turbine Double-Fed Induction Generator Based on Multi-Level Fusion and Measurement of Back-to-Back Converter Current Signal. *Iran. J. Electr. Electron. Eng.* **2022**, *18*, 2074. Available online: <http://ijeee.iust.ac.ir/article-1-2074-en.html> (accessed on 19 April 2022).